JOURNAL OF GEOPHYSICAL RESEARCH, VOL. 103, NO. C13, PAGES 30,793–30,812, DECEMBER 15, 1998

On tide propagation in convergent estuaries

Stefano Lanzoni

Dipartimento di Ingegneria Idraulica Marittima e Geotecnica, Università di Padova, Padua, Italy

Giovanni Seminara

Istituto di Idraulica, Università di Genova, Genoa, Italy

Abstract.

We revisit the problem of one-dimensional tide propagation in convergent estuaries considering four limiting cases defined by the relative intensity of dissipation versus local inertia in the momentum equation and by the role of channel convergence in the mass balance. In weakly dissipative estuaries, tide propagation is essentially a weakly nonlinear phenomenon where overtides are generated in a cascade process such that higher harmonics have increasingly smaller amplitudes. Furthermore, nonlinearity gives rise to a seaward directed residual current. As channel convergence increases, the distortion of the tidal wave is enhanced and both tidal wave speed and wave lenght increase. The solution loses its wavy character when the estuary reaches its "critical convergence"; above such convergence the weakly dissipative limit becomes meaningless. Finally, when channel convergence is strong or moderate, weakly dissipative estuaries turn out to be ebb dominated. In strongly dissipative estuaries, tide propagation becomes a strongly nonlinear phenomenon that displays peaking and sharp distortion of the current profile, and that invariably leads to flood dominance. As the role of channel convergence is increasingly counteracted by the diffusive effect of spatial variations of the current velocity on flow continuity, tidal amplitude experiences a progressively decreasing amplification while tidal wave speed increases. We develop a nonlinear parabolic approximation of the full de Saint Venant equations able to describe this behaviour. Finally, strongly convergent and moderately dissipative estuaries enhance wave peaking as the effect of local inertia is increased. The full de Saint Venant equations are the appropriate model to treat this case.

1. Introduction

This paper is focused on tide propagation in convergent estuaries. This subject has attracted the attention of several investigators owing to its relevance to the understanding of the behavior of many important real estuaries. Our interest in the problem also arises from the fact that the availability of a one-dimensional asymptotic theory of the hydrodynamics of tide propagation in convergent channels, extended to more than one dimension, can be set as the basis for investigations of tidal-induced transport of passive tracers or suspended sediments.

The first clear suggestion that in shallow estuaries the basic momentum balance differs from that characteristic of weakly dissipative estuaries and dominantly involves pressure gradient and friction was put forward by *Le Blond* [1978], who analyzed one-dimensional tidal propagation in a straight channel of uniform depth and width. *Le Blond* [1978] showed that as a result of the negligible role of local inertia, tide propagation in shallow estuaries behaves as a diffusive process rather than a hyperbolic wave. Furthermore, the horizontal length scale L_0^* of the tide propagation arising from momentum balance was shown to be much smaller than the frictionless tidal wavelength $\lambda^* \equiv T^*\sqrt{gD_0^*}$, where T^* is the tidal period, D_0^* is the average flow depth, and g is gravity (hereafter asterisks denote dimensional quantities). *Le Blond's* [1978] estimate for L_0^* reads

$$L_0^* = \sqrt{\frac{gD_0^{*2}T^*C_0^2}{U_0^*}} \tag{1}$$

where C_0 denotes a typical value of the flow conductance (i.e., the inverse square root of the friction coefficient c_D) while U_0^* is a characteristic amplitude of tidal velocity. The estimate (1), applied to two shallow estuaries, namely, the St. Lawrence and the Fraser, reveals that λ^* exceeds L_0^* by a factor of 3-5. The velocity scale U_0^* in the frictional regime of shallow estuar-

Paper number 1998JC900015.
0094-8276/98/1998JC900015$05.00

ies also differs significantly from the typical frictionless scale $\epsilon\sqrt{gD_0^*}$, with ϵ ratio between the characteristic tidal amplitude a^* and a typical flow depth D_0^*. The balance imposed by flow continuity in the case of a constant width gives

$$U_0^* = \epsilon\frac{L^*}{T^*} = \sqrt[3]{\frac{a^{*2}gC_0^2}{T^*}} \tag{2}$$

The picture changes considerably when the effect of estuary convergence is significant. About 160 years ago, *Green* [1837] employed an energy argument to treat tide propagation in estuaries with slowly varying width and depth in the absence of friction. The resulting Green's law predicts that tidal amplitude increases landward as $B^{*-1/2}D^{*-1/4}$, having denoted by B^* and D^* the local width and depth of the channel, respectively. However, both assumptions, slow channel convergence and frictionless propagation, are commonly nonrealistic, as the spatial scale of channel convergence is often much smaller than tidal wavelength while, most often, friction plays a nonnegligible or even dominant role in tide propagation. Let us then focus on two contributions that have recently attempted to remove the latter restrictions (but see *Jay* [1991] *and Friedrichs and Aubrey* [1994] for a detailed review of the previous literature).

Jay [1991] considered tide propagation in estuaries characterized by channel convergence, accounting for the presence of a steady river flow and for the retarding effect of tidal flats adjacent to the main channel treated as storage areas. Some finite amplitude effects were also accounted for, but the effect of overtides was not considered. As a result, the treatment of nonlinear terms of the momentum equation led to linear contributions and, not surprisingly, the resulting wave equation was indeed linear. *Jay* [1991] was then able to derive two analytical solutions: the former applies to weakly dissipative estuaries either strongly or weakly convergent, the latter concerns strongly dissipative estuaries. By analyzing the main features of his results, *Jay* [1991] was able to clarify how the classical picture associated with Green's solution is modified.

Jay's [1991] discussion centered on how the competing effects of local inertia, friction, and topography act to control the real and imaginary parts of the tidal wavenumber, hence of the wave speed and the rate of spatial growth or decay of tidal amplitude. In particular, it turned out that the topographic funneling effect predicted by Green may be significantly reduced or even overcome by damping associated with friction and using *Jay's* [1991] terminology, with "topography". (In our formulation we distinguish between the effects of "channel convergence", i.e., topographic funneling and the effect of along-channel gradients of tidal velocity, which is one of the actual sources of damping for the tidal wave).

A second interesting observation from *Jay's* [1991] results concerns the behavior of the tidal wave speed a, which was shown to depend strongly on the degree of channel convergence and on the intensity of friction. In particular, *Jay* [1991] defined a "critical convergence" such that the effects of local inertia and topography balanced exactly in his expression for the tidal wavenumber. For "subcritical convergent" estuaries the wave speed was found to decrease from the inviscid value $\sqrt{gD_0^*}$ as friction was increased. For "supercritically convergent" estuaries the wave speed was found to be linearly proportional to the ratio between convergence and friction and might attain very large values, while a phase difference between flow discharge and free surface elevation up to 90° was obtained.

Recently, *Friedrichs and Aubrey* [1994] reconsidered the case of strongly convergent shallow estuaries, suggesting that they are dynamically dominated by friction and kinematically controlled by convergence. In other words, in the context of *Friedrichs and Aubrey's* [1994] formulation, at the leading order of approximation, friction and gravity balance in the momentum equation, while, in the continuity equation, the net flux associated with channel convergence is required to balance the volumetric effect of temporal oscillations of free surface elevation. With the further help of the linearization of the frictional term, *Friedrichs and Aubrey* [1994], at the lowest order of approximation, derived a linearized kinematic wave equation, which they assumed to be the leading order approximation of the full de Saint Venant equations. The solution obtained in the context of such approximation has features that resemble those obtained in the classical theory of cooscillating tides, namely, negligible amplification of the tidal wave and relative phase between cross sectionally averaged velocity and free surface elevation of 90°. The latter similarities are in striking contrast with the fundamentally different nature of the two solutions, the former displaying the behavior of a frictionally dominated progressive wave, the latter consisting of a frictionless standing wave.

In the present contribution we revisit the subject of tide propagation in convergent channels considering four limit regimes identified by the degree of channel convergence and by the relative importance of friction as compared with local inertia. The results arising from our analysis add some interesting features to the previous picture. The first distinct feature, which does not seem to have been fully appreciated in the previous literature, is the conceptual and practical difference between the role of finite amplitude effects in weakly dissipative as opposed to strongly dissipative estuaries. In the former case, provided tidal amplitude is small compared with the mean flow depth, tide propagation is essentially a weakly nonlinear phenomenon; in other words, overtides of increasing order are generated in a cascade process such that their effect is decreasingly significant as their order increases. We are able to derive two perturbative weakly nonlinear solutions for tide propagation in weakly dissipative estuaries, either weakly or strongly convergent. Indeed, perturbation expan-

sions for the solution can be formally set up in terms of a small-amplitude parameter which allows a formally justified linearization of the frictional term. The resulting sequence of linear differential problems are then amenable to analytical treatment.

On the contrary, in strongly dissipative estuaries, tide propagation is a strongly nonlinear phenomenon; in other words, linearization of the frictional term is not justified even though a perturbation expansion can be still set up in terms of the small-amplitude parameter. We clarify this point by reexamining the kinematic wave approach appropriate to strongly convergent and strongly dissipative estuaries. In particular, we show that the solution of the fully nonlinear kinematic wave equation develops a discontinuity as a result of convergence of the characteristic lines arising when the nonlinear nature of the equation is preserved. We show that such discontinuity may be simply removed by keeping, at the leading order of approximation, the convective contribution in the continuity equation. The perturbation expansion set up for the solution allows us, at the leading order, to derive a nonlinear parabolic equation somewhat similar to that classically found in the context of the theory of flood propagation in rivers. By comparing the solution of the nonlinear parabolic model with the numerical solution of the complete de Saint Venant equations we find that, as expected, for given channel convergence measured by the dimensionless parameter K, the parabolic model is a good approximation of the full problem when the effect of local inertia in the momentum equation, measured by the dimensionless parameter S, is small enough. The two dimensionless parameters, S and K, are defined and discussed in section 2. As the role of local inertia increases, the diffusive effect introduced by the "parabolic" correction is counteracted; as a result, tide propagation experiences amplification and an enhanced tendency to wave peaking similar to that emerging in the context of the kinematic wave approximation.

A second feature arising from our work concerns the important question of flood versus ebb dominance. Weakly dissipative, moderately/strongly convergent estuaries are found to be ebb dominated as both the peak of ebb velocity and the duration of the ebb phase exceed the corresponding values for the flood phase. Furthermore, ebb dominance is increasingly displayed as channel convergence increases. However, notice that flood dominance is displayed by the temporal development of flow discharge. Furthermore, tidal propagation in weakly dissipative convergent estuaries gives rise to the generation of a seaward directed residual current superimposed on an otherwise symmetrical current profile.

On the contrary, strongly dissipative estuaries are invariably found to be flood dominated, a feature which will be seen to be associated with the process of peaking of the current profile that characterizes tide propagation in such estuaries. This latter feature also arose in the work of *Friedrichs and Aubrey* [1994]. However, we point out that our analysis does not cover the effect of the possible presence of tidal flats, which has been shown to be a cause of ebb dominance [*Speer and Aubrey*, 1985; *Friedrichs and Madsen*, 1992; *Shetye and Gouveia*, 1992].

Further features already emerged from the linearized treatment of *Jay* [1991] are confirmed by our analysis, as discussed in the next sections. The procedure followed in the rest of the paper is as follows. In the next section we formulate the mathematical problem of tide propagation in convergent estuaries. Section 3 is devoted to the limit behavior of weakly dissipative and weakly convergent estuaries. Section 4 treats the weakly dissipative and moderately or strongly convergent case. Highly dissipative estuaries are treated in section 5 for the weakly convergent case while, the effects of strong convergence are discussed in sections 6 and 7. Finally, section 8 is devoted a brief analysis of the important case of estuaries where the effects of local inertia are comparable with those of friction. Some discussion (section 9) concludes the paper.

2. Formulation of the Problem

We consider a straight channel closed at one end and connected at some initial cross section with a tidal sea. The channel is assumed to have length L_e^*, rectangular cross section with mean depth D_0^* and width $2B^*$ slowly varying in the longitudinal direction in the form (Figure 1)

$$B^* = B_0^* \exp\left(-\frac{x^*}{L_b^*}\right) \tag{3}$$

where x^* is longitudinal axis positive in the landward direction, B_0^* is half width of the channel at the entrance section where we set the origin of the x^* axis, and L_b^* is convergence length.

In the following we ignore the possible presence of tidal flats adjacent to the main channel and a mean

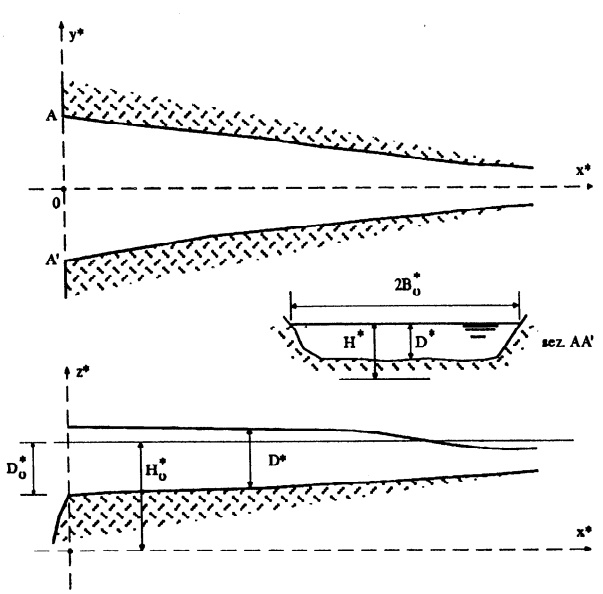

Figure 1. Sketch of the estuary.

depth variation along the estuary. In real estuaries the rate of channel convergence varies significantly. In fact, a measure of channel convergence is the quantity

$$\left|\frac{dB^*}{dx^*}\right| = \frac{B^*}{L_b^*} \tag{4}$$

Such ratio decreases in the longitudinal direction. For example in the case of the Delaware estuary it ranges about unity at the entrance but is reduced by 2 orders of magnitude at the inner end of the estuary and similarly for the Thames, where it is roughly reduced from 0.2 to 0.005.

Let a_0^* be a scale for the amplitude of free surface oscillations about the mean level, defined by the elevation H_0^*, and let D_0^* denote a scale for flow depth. We assume that, as is typical of many tidal environments, we can write

$$\epsilon = \frac{a_0^*}{D_0^*} \ll 1 \qquad \beta = \frac{B^*}{D_0^*} \gg 1 \tag{5}$$

Notice that ϵ typically keeps small along the whole estuary while β varies by orders of magnitude attaining values that may range from thousands at the mouth of the estuary to tenths at the inner end. The relevant physical quantities are then made dimensionless as follows:

$$D^* = D_0^* D \qquad x^* = L_0^* x \qquad t^* = \omega^{*-1} t$$
$$U^* = U_0^* U \qquad C = c C_0 \tag{6}$$

where ω^* is the angular frequency of the tidal wave, L_0^* is the length scale describing the typical spatial variations of the flow characteristics, C_0 is the characteristic value of flow conductance (inverse square root of friction coefficient) in the estuary, and U_0^* is the typical value of the cross sectionally averaged speed in the estuary.

It should be noted that the choice of any scaling quantity may not be uniformly valid either in space or in time. In particular, it will appear that the solution may tend to develop discontinuities, i.e., fairly sharp fronts; in a neighborhood of such fronts, spatial (or temporal) variations are obviously faster than those typically experienced by the tidal wave.

The appropriate choice for L_0^* and U_0^* in any specific context arises from the physical balances imposed by the equations of conservation of mass and momentum which, in dimensional form, read

$$D^*{}_{,t^*} + U^* D^*{}_{,x^*} + D^* U^*{}_{,x^*} - \frac{U^* D^*}{L_b^*} = 0 \tag{7}$$

$$U^*{}_{,t^*} + U^* U^*{}_{,x^*} + g D^*{}_{,x^*} + \frac{U^* |U^*|}{C^2 D^*} = 0 \tag{8}$$

where bed slope is taken as negligibly small.

Using the dimensionless variables defined by (6) and expanding D^* in the form

$$D^* = D_0^* [1 + \epsilon d(t, x) + O(\epsilon^2)] \tag{9}$$

with d an $O(1)$ quantity, the governing equations (7), (8) become

$$d_{,t} + \frac{F_0^2}{S\epsilon^2} (\epsilon U d_{,x} + D U_{,x}) - KUD = 0 \tag{10}$$

$$S U_{,t} + \frac{F_0^2}{\epsilon} U U_{,x} + d_{,x} + R \frac{U|U|}{c^2 D^{4/3}} = 0 \tag{11}$$

where we have set:

$$S = \frac{\omega^* L_0^*}{U_0^*} \frac{F_0^2}{c}, \quad R = \frac{F_0^2}{\epsilon} \frac{L_0^*}{C_0^2 D_0^*},$$
$$K = \frac{U_0^*}{\epsilon \omega^* L_b^*}, \quad C_0 = \frac{k_s}{\sqrt{g}} D_0^{*1/6} \tag{12}$$

and F_0 denotes the typical Froude number $U_0^*/\sqrt{g D_0^*}$, while k_s denotes Strickler coefficient, and Strickler's formula has been used to estimate the scale for conductance. Notice that the factor c is included to account for possible variations of flow conductance either in space (due to spatial variations of roughness) or in time (due to temporal variations possibly related to the presence of bed forms of varying amplitude). In the following, for the sake of simplicity, we will assume $c = 1$.

As already pointed out by several authors, besides the tidal amplitude parameter ϵ and the Froude number F_0, three major dimensionless parameters are found to play a fundamental role in tide propagation along a convergent estuary. The parameters S and R in the momentum equation denote, respectively, a measure of the effect of local inertia and friction relative to that of gravity, while the parameter K occurring in the continuity equation measures the kinematic effect of topography (channel convergence) relative to the effect of temporal oscillations of free surface elevation.

On the basis of the values attained by the above parameters, we may then classify estuaries as weakly (strongly) convergent if $K \ll 1 (K \sim O(1))$ and weakly (strongly) dissipative if $R/S \ll 1 (R/S \gg 1)$. Notice that the ratio R/S reads $U_0^*/\omega^* C_0^2 D_0^*$, hence it is independent of the spatial scale L_0^* and may be readily estimated for the estuaries reported in Table 1. The values of the dimensionless parameters ϵ, K, and R/S reported in Table 2 show that a wide variety of estuary types is indeed found in nature. Basically, one may recognize the following four limiting behaviors of tide propagation: (1) weakly dissipative and weakly convergent (WD-WC), (2) weakly dissipative and strongly convergent (WD-SC), (3) strongly dissipative and weakly convergent (SD-WC), and (4) strongly dissipative and strongly convergent (SD-SC). In the following we attempt to formulate appropriate nonlinear models for each of these limiting behaviors.

It was suggested by D.A. Jay that it might be helpful to rescale (10) and (11) by referring to the classical scaling employed in the context of inviscid tide propagation in constant width channels. This can be done by expressing the length scale L_0^* and the velocity scale U_0^* in the form

$$L_0^* = \frac{\sqrt{g D_0^*}}{\omega^*} \psi, \qquad U_0^* = \epsilon \sqrt{g D_0^*} \phi \tag{13}$$

Table 1. Observed tidal and geometric properties of various tidal estuaries

Estuary	a_0^*, m	$T^*, hours$	L_e^*, Km	L_b^*, Km	D_0^*, m	$U_0^*, m/s$	C_0	source
Bristol Channel	2.60	12.4	80	65	45.0	1.0	20.0	1
Columbia[a]	1.00	12.4	240	25	10.0	1.0	18.0	2
Conwy	2.40	12.5	22	6.3	3.0	0.5	14.0	3
Delaware	0.64	12.5	215	40	5.8	0.6	21.8	4
Elbe[a]	2.00	12.4	77	42	10.0	1.0	20.0	5
Fleet	0.60	12.5	12.5	-	1.5	0.4	22.4	6
Fraser[a]	1.50	12.4	108	215	9.0	1.0	14.4	7
Outer Bay of Fundy	2.10	12.4	190	230	60.0	1.0	21.0	8
Gironde[b]	2.30	12.4	77	44	10.0	1.0	18.0	9
Hoogly	2.10	12.0	72	25.5	5.9	-	-	10
Hudson	0.69	12.4	245	140	9.2	0.7	30.9	11
Irrawaddy	1.00	12.0	124	35	12.4	-	-	10
Khor[b]	1.30	12.0	90	20.6	6.7	-	-	10
Ord	2.50	12.0	65	15.2	4.0	2.0	20.0	10
Potomac	0.65	12.4	184	54	6.0	0.9	24.0	11
Rotterdam Waterway	1.00	12.4	37	56	11.5	0.7	21.0	12
Scheldt	1.90	12.4	77	54	8.0	0.5	16.5	13
Severn	3.00	12.4	110	41	15.0	1.5	20.0	1
Soirap	1.30	12.0	95	34	7.9	-	-	10
St. Lawrence[a]	2.50	12.4	330	183	7.0	1.0	28.8	14
Tamar	2.60	12.5	21	4.6	2.9	0.5	25.0	4
Tees	1.50	12.0	14	5.5	7.5	0.4	16.0	15
Thames	2.00	12.3	95	25	8.5	0.6	14.1	4

Sources: 1, *Uncles* [1981], [1991]; 2, *Giese and Jay* [1989]; 3, *Wallis and Knight* [1984], *Knight* [1981]; 4, *Friedrichs and Aubrey* [1994]; 5, *Duwe and Sundermann* [1986]; 6, *Robinson et al.* [1983], *Shetye and Gouveia* [1992]; 7, *Ages and Woollard* [1976], *Le Blond* [1978]; 8, *Greenberg* [1979]; 9, *Allen et al.* [1980]; 10, *Wright et al.* [1973]; 11, *Thatcher and Harleman* [1972]; 12, *Abraham et al.* [1986]; 13, *de Jong and Gerritsen* [1984]; 14, *Prandle and Crookshank* [1974], *Le Blond* [1978]; 15, *Lewis and Lewis* [1987]. Parameters are defined in the text.

[a]Fluvially influenced estuaries.

[b] Extreme annual variability of the freshwater discharge.

where ψ and ϕ are parameters which keep $O(1)$ only in the weakly dissipative and weakly convergent case.

Simple algebraic manipulations then lead to the following structure of the continuity and momentum equations:

$$d_{,t} + \frac{\phi}{\psi}(\epsilon U d_{,x} + D U_{,x}) - K_0 \phi U D = 0 \qquad (14)$$

$$(\phi\psi) U_{,t} + (\epsilon\phi^2) U U_{,x} + d_{,x} + (\epsilon\phi^2\psi R_0)\frac{U|U|}{c^2 D^{4/3}} = 0 \qquad (15)$$

where

$$K_0 = \frac{\sqrt{g D_0^*}}{\omega^* L_b^*}, \qquad R_0 = \frac{\sqrt{g D_0^*}}{\omega^* C_0^2 D_0^{*4/3}} \qquad (16)$$

This formulation unambiguously clarifies that only three parameters control tide propagation in estuaries. Indeed, the forms of ϕ and ψ appropriate to each of the limiting behaviors discussed in this paper depend on the three parameters, ϵ, K_0, and R_0. In the following, however, we will keep the formulation (10) and (11) which we feel to be less cumbersome for the reader, but we will point out the equivalent choices for ϕ and ψ appropriate to each of the limiting case examined below.

Furthermore, we restrict our attention to the case of a simple harmonic tidal wave by assuming at the outlet of the estuary:

$$d|_{x=0} = \cos t \qquad (17)$$

At the upstream end of the estuary we may either assume that the tidal wave decays asymptotically as x increases (river channels) or that complete reflection (i.e., $U|_{x=x_L} = 0$) occurs at some tidal barrier (closed channel). Herein, for the sake of simplicity we adopt the former condition in the analytic treatment of the first two cases (WD-WC and WD-SC), while the condition $U|_{x=x_L} = 0$ has been adopted in the numerical calculations pertinent to the latter two cases (SD-WC and SD-SC). Notice that the tidal barrier condition would be easily applied in the former case as well. On the other hand, the numerical calculations carried out by *Parker* [1991] have shown that the effects of an increasingly high river discharge (i.e., $U|_{x=x_L} < 0$) remain localized (at least as far as the fundamental M_2 tide is concerned) within the upper reach of the estuary. Therefore the choice of the boundary conditions herein pursued is not likely to affect substantially the results presented in the following sections.

Table 2. Dimensionless parameters characterizing the tidal estuaries of Table 1

Estuary	ϵ	K	R/S	Type
Bristol Channel	0.07	1.68	0.44	SC - WD
Columbia	0.10	2.84	2.19	SC - SD
Conwy	0.80	0.71	6.09	MC - SD
Delaware	0.11	0.97	1.55	SC - MD
Elbe	0.20	0.85	1.78	MC - SD
Fleet	0.40	0.02	3.81	WC - SD
Fraser	0.17	0.20	3.81	WC - SD
Outer Bay of Fundy	0.04	0.88	0.30	MC - WD
Gironde	0.23	0.70	2.19	MC - SD
Hoogly [a]	0.36	0.76	2.91	MC - SD
Hudson	0.08	0.50	0.60	MC - MD
Irrawaddy [a]	0.08	2.44	1.39	SC - MD
Khor [a]	0.19	1.73	2.55	SC - SD
Ord [a]	0.62	1.45	8.59	SC - SD
Potomac	0.11	1.09	1.85	SC - MD
Rotterdam Waterway	0.09	1.02	0.98	SC - MD
Scheldt	0.24	0.28	1.63	WC - MD
Severn	0.15	1.73	1.33	SC - MD
Soirap [a]	0.16	1.23	2.18	SC - SD
StLawrence	0.36	0.11	1.22	WC - MD
Tamar	0.90	0.87	1.98	MC - SD
Tees	0.20	2.50	1.43	SC - MD
Thames	0.24	0.78	2.71	MC - SD

Abbreviations: SC, strongly convergent; MC, moderately convergent; WC, weakly convergent; SD, strongly dissipative; MD, moderately dissipative; WD, weakly dissipative. Parameters are defined in the text.

[a]The value of U_0 and C_0 could not be inferred from the source and the values of the parameters have been evaluated by arbitrarily assuming $U_0 = 1$ m/s and $C_0 = 20$.

3. Weakly Dissipative and Weakly Convergent Estuaries

An example of such an estuary is the seaward portion of the bay of Fundy, which is characterized by a nearly rectangular geometry in plane view and, owing to the large depths (of the order of some tens of meters), by a fairly low friction coefficient [*Greenberg*, 1979, *Prandle and Rahman*, 1980].

This limiting behavior is mathematically described by the following conditions

$$\frac{R}{S} \ll 1 , \qquad K \ll 1 \tag{18}$$

Momentum conservation here requires that local inertia must dominantly balance gravity while, neglecting the topographic effect, flow continuity leads to a balance between first and second terms in (10). It is then convenient to set

$$S = 1 , \qquad \frac{F_0^2}{\epsilon^2 S} = 1 , \tag{19}$$

which, recalling (12), is equivalent to the following choice of the scales L_0^* and U_0^*:

$$L_0^* = \frac{\sqrt{gD_0^*}}{\omega^*} , \qquad U_0^* = \epsilon\sqrt{gD_0^*} \tag{20}$$

We point out that in terms of the alternative formulation (14) and (15) the above scaling corresponds to choosing $\phi = \psi = 1$ in (13).

Also note that (19) imply that $F_0^2 \sim O(\epsilon^2)$, hence convective inertia is also negligible in the momentum equation. At this stage it is convenient to expand

$$U = U_0 + \epsilon U_1 + O(\epsilon^2) , \tag{21}$$

$$d = d_0 + \epsilon d_1 + O(\epsilon^2) . \tag{22}$$

At leading order substitution of (21) and (22) into (10) and (11) leads to the classical linear scheme of tide propagation in inviscid rectangular channels:

$$d_{0,t} + U_{0,x} = 0 , \tag{23}$$

$$d_{0,x} + U_{0,t} = 0 . \tag{24}$$

Provided no reflection of the tidal wave occurs the general solution of (23) and (24) may be set in the form

$$[U_0, d_0] = \sum_{m=1}^{\infty} \{[\phi_{m1}(\xi), \mathcal{D}_{m1}(\xi)] \cos m(x-t) + [\phi_{m2}(\xi), \mathcal{D}_{m2}(\xi)] \sin m(x-t)\} , \tag{25}$$

where, using the language of the multiple scale technique [*Nayfeh*, 1973, p. 49], ξ is a "slow" spatial variable, defined as

$$\xi = \epsilon x , \tag{26}$$

which describes a weak modulation of the amplitude of the tidal wave associated with the effects of channel convergence and friction.

Substituting from (25) into (23) and (24), we readily find

$$\phi_{mi} = \mathcal{D}_{mi} \qquad (i = 1, 2; m = 1, 2, ...) . \tag{27}$$

Notice that (27) suggests that, as is well known, in weakly dissipative and weakly convergent estuaries of infinite length, velocity is dominantly in phase with free surface elevation. Having assumed that both convergence and dissipation are weak, let us set

$$K = k\epsilon , \qquad R = r\epsilon . \tag{28}$$

Substituting from (21) and (22) into (10) and (11), using (28) and the chain rule

$$\frac{\partial}{\partial x} \to \frac{\partial}{\partial x} + \epsilon \frac{\partial}{\partial \xi} , \tag{29}$$

at $O(\epsilon)$ we find

$$d_{1,t} + U_{1,x} = -(d_0 U_0)_{,x} + kU_0 - U_{0,\xi} , \tag{30}$$

$$U_{1,t} + d_{1,x} = -rU_0|U_0| - d_{0,\xi} - \left(\frac{1}{2}U_0^2\right)_{,x} . \tag{31}$$

¿From (30) and (31) we readily obtain a second-order

linear partial differential equation governing the function $d_1(x,t)$:

$$d_{1,tt} - d_{1,xx} = -(d_0 U_0)_{,xt} + kU_{0,t} - U_{0,\xi t} + r(U_0|U_0|)_{,x} + d_{0,\xi x} + \left(\frac{1}{2}U_0^2\right)_{,xx} . \quad (32)$$

Equation (32), like the system (23) and (24) is hyperbolic. Recalling (17), it follows that

$$\mathcal{D}_{11}|_{\xi=0} = 1; \qquad \mathcal{D}_{m1}|_{\xi=0} = 0 \quad (m > 1);$$
$$\mathcal{D}_{m2}|_{\xi=0} = 0 \quad (m \geq 1) . \quad (33)$$

Since, at leading order, U_0 is equal to $\mathcal{D}_{11}(\xi)\cos(x-t)$ (as $\mathcal{D}_{22}$ and $\mathcal{D}_{31}$ keep $O(\epsilon)$ along the estuary) and $\mathcal{D}_{11}$ keeps positive, a classical expansion truncated at second order gives

$$U_0|U_0| = \left[\frac{8}{3\pi}\cos(x-t) + \frac{8}{15\pi}\cos 3(x-t) + ...\right]\mathcal{D}_{11}^2 . \quad (34)$$

Now it should be noticed that each of the terms at the right-hand side of (32) is secular; indeed, any of these terms would lead to solutions for d_1 proportional to $x\cos m(x-t)$ (or $x\sin m(x-t)$) for some m, and such solutions are unbounded for $x \to \infty$. Hence the right-hand side of (32) must vanish. This condition implies

$$\frac{d\mathcal{D}_{11}}{d\xi} = -\frac{4}{3}\frac{r}{\pi}\mathcal{D}_{11}^2 + \frac{k}{2}\mathcal{D}_{11} , \quad (35)$$

$$\frac{d\mathcal{D}_{22}}{d\xi} = \frac{3}{4}\mathcal{D}_{11}^2 , \quad (36)$$

$$\frac{d\mathcal{D}_{31}}{d\xi} = -\frac{4r}{15\pi}\mathcal{D}_{11}^2 , \quad (37)$$

Equation (35) shows that the amplitude of the fundamental may either decay of grow, depending on the balance between channel convergence and friction. Indeed, we find

$$\mathcal{D}_{11} = \frac{c_s \exp(k\xi/2)}{1 + \mathcal{B}c_s \exp(k\xi/2)} ; \qquad c_s = \frac{1}{1-\mathcal{B}} ;$$
$$\mathcal{B} = \frac{8}{3\pi}\frac{r}{k} . \quad (38)$$

It is easy to show that $\mathcal{D}_{11}$ keeps constant whenever the following condition is satisfied:

$$\frac{k}{r} = \frac{C_0^2 D_0^*}{\epsilon L_b^*} = \frac{8}{3\pi} , \quad (39)$$

i.e., whenever the 'Green' amplification effect associated with topographic funneling is exactly balanced by friction.

Evaluating the functions $\mathcal{D}_{22}$ and $\mathcal{D}_{31}$ requires some straightforward algebraic work to integrate equations (36) and (37). We find

$$(\mathcal{D}_{22}, \mathcal{D}_{31}) = \left(\frac{3}{4}, -\frac{4}{15}\frac{r}{\pi}\right)\mathcal{D}(\xi) , \quad (40)$$

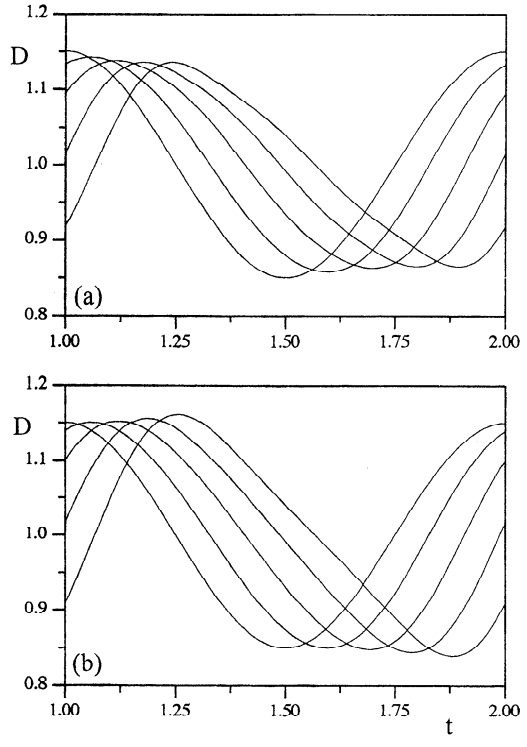

Figure 2. Time evolution of the dimensionless flow depth $D = D^*/D_0^*$ at distances $x^*/L_e^* = m/4$ ($m = 0, 4$) from the outlet of the estuary as predicted by (42). The values of the adopted parameters, typical of a weakly dissipative and weakly convergent estuary, are (a) $\epsilon = 0.15$, $S = 1$, $K = 0.15$, $R = 0.4$, $L_e^*/L_0^* = 2$, and (b) $\epsilon = 0.15$, $S = 1$, $K = 0.3$, $R = 0.15$, $L_e^*/L_0^* = 2$.

where

$$\mathcal{D}(\xi) = \frac{2}{k}\frac{1}{\mathcal{B}^2}\left\{\ln\left[\frac{1+\mathcal{B}c_s\exp(k\xi/2)}{1+\mathcal{B}c_s}\right] + \frac{1}{1+\mathcal{B}c_s\exp(\xi k/2)} - \frac{1}{1+\mathcal{B}c_s}\right\} . \quad (41)$$

Summarizing, the complete solution for D up to $O(\epsilon)$ reads

$$D = 1 + \epsilon[\mathcal{D}_{11}(\xi)\cos(x-t) + \mathcal{D}_{22}(\xi)\sin 2(x-t) + \mathcal{D}_{31}(\xi)\cos 3(x-t)] + O(\epsilon^2) . \quad (42)$$

The temporal development of the solution for D at various cross sections along the estuary is plotted in Figure 2.

In order to complete the derivation of the solution up to $O(\epsilon)$, we need to calculate U_1. It is easy to show that an equation similar to that obtained for d_1 is derived for U_1 from (30) and (31). Suppressing secular terms, such equation becomes

$$U_{1,xx} + U_{1,tt} = 0 \quad (43)$$

Notice that (43) must be solved requiring that the net flow discharge in a tidal cycle must vanish at any order. Hence, denoting by angle brackets the average over a cycle, we must require that

$$\langle UD \rangle = \langle U_0 \rangle + \epsilon \langle U_0 d_0 + U_1 \rangle + O(\epsilon^2) = 0 \qquad (44)$$

Recalling the expressions for U_0 and d_0, it follows that the solution for U_1 must read

$$U_1 = -\frac{1}{2}\left(\mathcal{D}_{11}^2 + \mathcal{D}_{22}^2 + \mathcal{D}_{31}^2\right) + \Phi_1(x,t;\xi) \qquad (45)$$

where Φ_1 is a periodic function, of the form (25), which is needed to suppress secular terms at order ϵ^2. Below we do not pursue the evaluation of Φ_1, which would only provide weak corrections to the harmonic content of U_0. However, it is of interest to note that the effect of the first term on the right-hand side of (45) is to give rise to a weak residual current needed to satisfy global continuity. Furthermore, the solution for U suggests that, at least at the leading order, weakly dissipative and weakly convergent estuaries are neither ebb dominated, nor flood dominated.

The above analysis applies within most of the upper central region of Figure 2 and 3 of *Jay* [1991]. The present weakly nonlinear extension shows that the effect of weak nonlinearities associated with friction and spatial nonuniformity of velocity and depth gives rise at second order to an M_4 correction of the fundamental (M_2) along with a much weaker M_6 correction and a negative residual current.

A perturbation analysis somewhat related to that presented in this section was proposed by Kreiss [1957]. However, in such work, neither convergence nor friction nonlinearity was taken into account.

4. Weakly Dissipative and Moderately or Strongly Convergent Estuaries

We now move to the upper right region of Figure 2 and 3 of *Jay* [1991]; in other words, we consider estuaries weakly affected by friction and moderately or strongly convergent, in the sense that both K and $(F_0^2/\epsilon^2 S)$ are $O(1)$ quantities. Among the estuaries collected in Table 1, only the Bristol Channel satisfies the latter condition. Anyhow, it is of interest to examine this limiting behavior as part of the complete picture that we wish to draw.

In the present case it is convenient to set

$$S = 1 \,, \qquad K = 1 \,. \qquad (46)$$

Recalling (12), the conditions (46) are readily shown to be equivalent to the following choice of the spatial and velocity scales L_0^* and U_0^*:

$$U_0^* = \epsilon \omega^* L_b^* \,, \qquad L_0^* = \frac{g D_0^*}{\omega^{*2} L_b^*} \,. \qquad (47)$$

Furthermore, neglecting dissipation at leading order formally requires that the ratio R/S be small. We point out that, in terms of the formulation (13) the scaling (47) is readily shown to correspond to choosing $\phi = 1/K_0$ and $\psi = K_0$.

Substituting from the expansions (21) and (22) into (10) and (11) with R expressed in the form (28), at leading order we find:

$$d_{0,t} + \mathcal{F} U_{0,x} - U_0 = 0 \,, \qquad (48)$$

$$U_{0,t} + d_{0,x} = 0 \,, \qquad (49)$$

having defined

$$\mathcal{F} = \frac{F_0^2}{\epsilon^2} = \frac{L_b^*}{L_0^*} \,. \qquad (50)$$

¿From (48) and (49) we readily derive the following linear second-order partial differential equation of hyperbolic type for d_0:

$$\mathcal{F} d_{0,xx} - d_{0,x} - d_{0,tt} = 0 \,. \qquad (51)$$

Recalling the boundary condition (17), (49) and (51) are solved in the form

$$d_0 = \exp\left(\frac{x}{2\mathcal{F}}\right)\left[\frac{1}{2}\exp i(t - \lambda_1 x) + \text{c.c.}\right] \,, \qquad (52)$$

$$U_0 = \exp\left(\frac{x}{2\mathcal{F}}\right)\left[(\gamma_0 + i\gamma_1)\exp i(t - \lambda_1 x) + \text{c.c.}\right] \qquad (53)$$

where c.c. denotes the complex conjugate of a complex number. Furthermore, γ_0 and γ_1 read

$$\gamma_0 = \frac{\lambda_1}{2} \,, \qquad \gamma_1 = \frac{1}{4\mathcal{F}} \,, \qquad (54)$$

$$\lambda_1 = \frac{\sqrt{4\mathcal{F} - 1}}{2\mathcal{F}} \,, \qquad (55)$$

having assumed that $\mathcal{F}$ keeps larger than 1/4.

The latter solution displays most of the features pointed out by *Jay* [1991]. In particular, it loses its wavy character when the condition $\mathcal{F} = 1/4$ is satisfied; this is the condition called critical convergence by *Jay* [1991]. Recalling (47) and (50), the latter condition occurs, provided

$$L_b^* = \frac{\sqrt{g D_0^*}}{2\omega^*} \,. \qquad (56)$$

Notice that, as pointed out by *Lighthill* [1978], the supercritical regime $\mathcal{F} < 1/4$ is meaningless in the inviscid limit. Also notice that, in agreement with *Jay* [1991], both the wavelength and the wave speed increase very rapidly in the subcritical regime $\mathcal{F} > 1/4$ close to criticality. Finally, since the rate of width reduction can be written in this case in the form $B_0^* \exp(-x/\mathcal{F})$, at leading order the flow discharge in the subcritical regime decays exponentially in spite of the exponential growth of the tidal velocity.

Let us proceed to $O(\epsilon)$. Substituting from the expansions (21), (22), and (28) into (10) and (11), and recalling (46), at $0(\epsilon)$ we find

$$U_{1,t} + d_{1,x} = -r U_0 |U_0| - \frac{\mathcal{F}}{2}(U_0^2)_{,x} \,, \qquad (57)$$

$$d_{1,t} + \mathcal{F} U_{1,x} - U_1 = -\mathcal{F}(d_0 U_0)_{,x} + (d_0 U_0) \,, \qquad (58)$$

hence

$$\begin{aligned} \mathcal{F}d_{1,xx} &- d_{1,x} - d_{1,tt} = -r\mathcal{F}[U_0|U_0|]_{,x} + rU_0|U_0| \\ &+ \frac{\mathcal{F}}{2}(U_0^2)_{,x} - \frac{\mathcal{F}^2}{2}(U_0^2)_{,xx} \\ &+ \mathcal{F}(d_0U_0)_{,xt} - (d_0U_0)_{,t} \ . \end{aligned} \tag{59}$$

In order to proceed analytically, we employ *Dronkers'* [1964] approach to expand the quantity $U_0|U_0|$.

Let us denote by U_a the maximum value of U_0. Recalling (53), it is easy to show that such a maximum occurs when the following condition is satisfied:

$$t - \lambda_1 x = \arctan\left(-\frac{1}{2\mathcal{F}\lambda_1}\right) \ , \tag{60}$$

the solution in the fourth quadrant being the appropriate one. Hence we readily find

$$U_a = \hat{U}_a \exp\left(\frac{x}{2\mathcal{F}}\right) \ , \ \hat{U}_a = \frac{\sqrt{1+4\mathcal{F}^2\lambda_1^2}}{2\mathcal{F}} \ . \tag{61}$$

Dronkers [1964] has shown that the term $U_0|U_0|$ with U_0 periodic function with zero mean and maximum value $U_a(x)$ may be expanded, using Chebyshev polynomials as follows

$$U_0|U_0| = \frac{16}{15\pi}U_a^2\left[\frac{U_0}{U_a} + 2\left(\frac{U_0}{U_a}\right)^3\right] \ . \tag{62}$$

Using the latter approximation and the solution (52) and (53) for d_0 and U_0, some tedious algebra allows us to evaluate d_1 in the form

$$\begin{aligned} d_1 &= \sum_{m=1}^{3} \Delta_m \left[-\exp\left(\frac{x}{2\mathcal{F}}\right)\exp i(mt - \lambda_m x)\right. \\ &+ \left.\exp\left(\frac{x}{\mathcal{F}}\right)\exp im(t-\lambda_1 x) + \text{c.c.}\right] \\ &+ d_{10}\left[\exp\left(\frac{x}{\mathcal{F}}\right) - 1\right] \end{aligned} \tag{63}$$

The coefficients $\Delta_1, \Delta_2, \Delta_3$ are given in the appendix, while the constant d_{10} is evaluated below by suppressing secular terms that would otherwise arise in the solution for U_1. Furthermore, the quantities λ_2 and λ_3 read

$$\lambda_2 = \frac{\sqrt{16\mathcal{F}-1}}{2\mathcal{F}} \ , \qquad \lambda_3 = \frac{\sqrt{36\mathcal{F}-1}}{2\mathcal{F}} \ . \tag{64}$$

Further algebra allows us to solve equation (57) for U_1 using the solution (63) for d_1. We find

$$\begin{aligned} U_1 &= u_{10}(x) + \sum_{m=1}^{3}\left[\exp\left(\frac{x}{2\mathcal{F}}\right)\phi_m \exp im(t-\lambda_1 x)\right. \\ &+ \left.\exp\left(\frac{x}{\mathcal{F}}\right)\varphi_m \exp i(mt-\lambda_m x) + \text{c.c.}\right] \ , \end{aligned} \tag{65}$$

where ϕ_m and φ_m are constants given in the appendix. Furthermore, the constant d_{10} of (63) must take the value

$$d_{10} = -\mathcal{F}(\gamma_0^2 + \gamma_1^2) \ , \tag{66}$$

to avoid the occurrence of a secular term (linear in time) which arises from the effect of convective inertia. Finally, the function $u_{10}(x)$ is evaluated by imposing vanishing flow discharge averaged over a cycle (see (44)). Employing the solutions for U_0, d_0 and U_1, the latter condition gives

$$u_{10} = -\gamma_0 \exp\left(\frac{x}{\mathcal{F}}\right) \tag{67}$$

The picture arising from the above results is as follows. The linear behavior of weakly dissipative estuaries in the moderately strongly convergent limit confirms *Jay's*

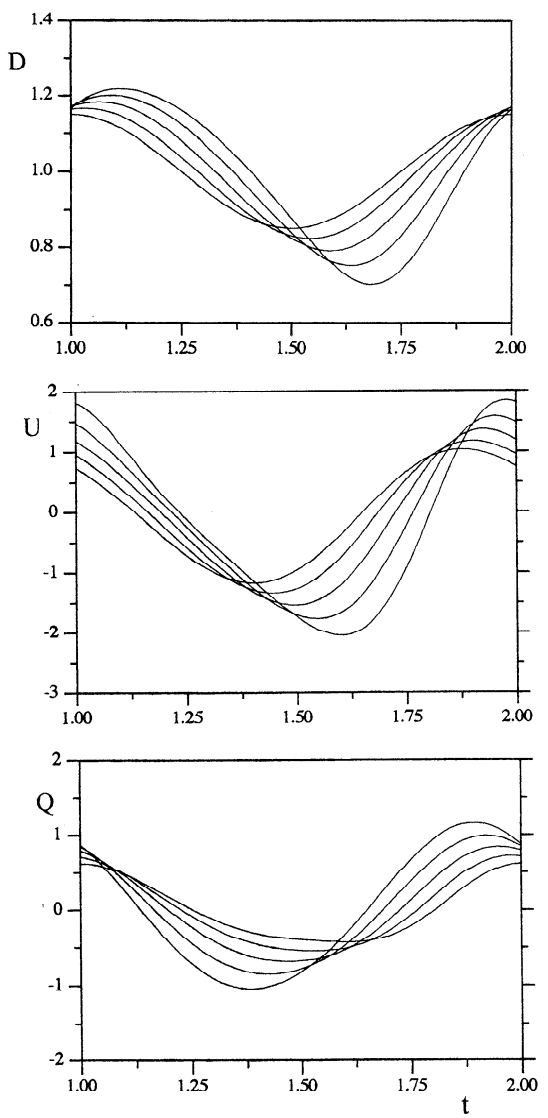

Figure 3. Time evolution of the dimensionless flow depth $D = D^*/D_0^*$, tidal velocity $U = U^*/U_0^*$, and flow discharge $Q = Q^*/(B_0^*D_0^*U_0^*)$ at distances $x^*/L_e^* = m/4$ $(m = 0, 4)$ from the outlet of the estuary as predicted by (52) and (53) along with (63) and (65). The values of the adopted parameters, typical of a weakly dissipative and moderately convergent estuary, are $\epsilon = 0.15$, $S = 1$, $K = 1$, $R = 0.15$, $\mathcal{F} = 0.8$, $L_e^*/L_0^* = 1$.

[1991] results. In particular the wave amplifies landward and both its wavelength and wave speed increase rapidly close to the critical convergence of *Jay* [1991] (see (55)). Furthermore, the latter equation shows that the phase lag between flow depth and tidal velocity increases from the vanishing weakly convergent limit ($\gamma_1 \to 0$ as $\mathcal{F} \to \infty$) to 90° as the critical convergence limit is approached ($\gamma_1 \to 1$ as $\mathcal{F} \to 1/4$). Similarly, as $\mathcal{F} \to \infty$, the amplitude of tidal velocity γ_0 behaves as $1/2\sqrt{\mathcal{F}}$ while the tidal wavenumber tends to $1/\sqrt{\mathcal{F}}$. Recalling that our scaling (47) involves L_b^*, one can readily show that such limits coincide with the corresponding values obtained in the weakly dissipative case.

Nonlinearity arising from convective inertia and channel convergence gives rise to the development of an M_4 tidal component while friction nonlinearity produces a correction of the fundamental M_2 and a third harmonic (M_6). Overtides amplify in the landward direction, and their rate of amplification is twice as fast as that characterizing the fundamental. Hence the profile of the tidal wave is increasingly distorted, as Figure 3 shows. A second effect of nonlinearity is the development of a progressive lowering of the mean water level in the landward direction along with a negative residual current. As a result, weakly dissipative and moderately/strongly convergent estuaries appear to be ebb dominated, in the sense that both the peak of ebb velocity and the duration of the ebb phase exceed the corresponding values for the flood phase. Nevertheless, the flow discharge (see Figure 3) exhibits a larger peak during the flood period since water level and velocity are about in phase.

5. Strongly Dissipative and Weakly Convergent Estuaries

We now assume that gravity and friction dominate momentum balance, that is, local inertia is relatively small and channel convergence is weak. These conditions are satisfied for the Fleet and the Fraser estuaries. It is then convenient to set

$$R = 1 , \qquad \frac{F_0^2}{\epsilon^2 S} = 1 , \tag{68}$$

and, recalling (12), the following scales for L_0^* and U_0^* emerge:

$$L_0^* = \left(\frac{C_0^2 g D_0^{*2}}{\omega^{*2} \epsilon} \right)^{1/3} ,$$
$$U_0^* = (\omega^* \epsilon^2 g C_0^2 D_0^{*2})^{1/3} . \tag{69}$$

Note that the condition of negligible local inertia implies that S/R be small. Also, in terms of the formulation (13) the scales (69) are equivalent to choosing both ϕ and ψ equal to $(\epsilon R_0)^{-1/3}$.

The scaling (69) appears to estimate the actual intensity of tidal velocity for the Fleet and Fraser estuaries (see Table 1) fairly well, as we find $U_0^* = 0.63$ m/s for the Fleet estuary and $U_0^* = 0.86$ m/s for the Fraser estuary. Also note that an estimate of U_0^* based on the classical weakly dissipative scheme (see (20)) would sharply overestimate U_0^* (1.53 m/s for the Fleet and 1.57 m/s for the Fraser). An expansion of the usual form (21) and (22) then leads to the following problem at leading order:

$$d_{0,t} + U_{0,x} = 0 , \tag{70}$$
$$d_{0,x} + U_0 |U_0| = 0 , \tag{71}$$

or, after simple manipulations,

$$U_{0,xx} - (U_0 |U_0|)_{,t} = 0 . \tag{72}$$

The latter equation is a quasi-linear second-order partial differential equation of parabolic type that describes a diffusive behavior of the tidal wave.

Unfortunately, (72) cannot be solved analytically unless the frictional term is linearized. A linearized treatment has been recently proposed by *Friedrichs and Madsen* [1992]. However, linearization may be justified only in relatively short estuaries such that nonlinear effects cannot fully develop. Otherwise, as it is shown below, linearization severely affects the behavior of the solution. We then defer the treatment of this case to the next sections, where it is treated as a particular case of the strongly dissipative and strongly convergent case.

6. Strongly Dissipative and Strongly Convergent Estuaries: the Kinematic Wave Approach

We now assume that local inertia is small relative to dissipation and convergence is strong. Hence we set

$$R = 1 , \qquad K = 1 , \tag{73}$$

which correspond to the following choice of the relevant scales:

$$U_0^* = \epsilon \omega^* L_b^* , \qquad L_0^* = \frac{g D_0^{*2} C_0^2}{\epsilon \omega^{*2} L_b^{*2}} . \tag{74}$$

In terms of the formulation (13) the latter scaling is equivalent to choosing $\phi = 1/K_0$ and $\psi = K_0^2/(\epsilon R_0)$.

Table 1 shows that several estuaries may be taken to approximate the above scheme, though, actually, the effect of local inertia is seldom small. Estimates for U_0^* based on (74) give 0.35, 0.70, 1.13, 1.42, 1.38, 0.57, and 0.83 m/s, respectively, for the Columbia, Conwy, Elbe, Gironde, Ord, Tamar, and Thames estuaries which most closely fit the strongly dissipative and strongly convergent scheme. Again, notice that the weakly dissipative estimate (20) would usually overestimate strongly the above values (0.99, 4.34, 1.98, 2.28, 3.91, 4.78, and 2.15 m/s, respectively, for each of the above estuaries). We can then attempt to solve the problem analytically by setting the usual asymptotic expansion (21) and (22) for d and U in terms of the

small parameter ϵ. From (74) and the definition of S it follows that

$$S = \frac{D_0^* C_0^*}{\epsilon L_b^*} , \qquad \frac{F_0^2}{\epsilon^2 S} = \mathcal{F} = \frac{L_b^*}{L_0^*} \tag{75}$$

Let us then assume that S and $\mathcal{F}$ are both of order ϵ and substitute from (21), (22), and (73), into (10) and (11). At leading order, we find the following equations:

$$d_{0,t} - U_0 = 0 , \tag{76}$$

$$d_{0,x} + U_0|U_0| = 0 . \tag{77}$$

The latter system is readily reduced to the following nonlinear first-order partial differential equation for d_0:

$$d_{0,x} + d_{0,t}|d_{0,t}| = 0 . \tag{78}$$

Equation (78) may be transformed into a kinematic wave equation that reads

$$d_{0,t} + a(t) d_{0,x} = 0 , \tag{79}$$

where $a(t)$ is a dimensionless wave speed such that

$$a(t) = \frac{1}{|d_{0,t}|} . \tag{80}$$

The above approach is similar to that proposed by *Friedrichs and Aubrey* [1994]. However, from (80) it is apparent that the local value of the wave speed varies from some finite value to infinity at any cross section where the derivative $d_{o,t}$ vanishes instantaneously. Hence, in the context of the latter approximation, the tidal wave is subject to the process of peaking typical of kinematic waves characterized by convergence of the characteristic lines, which leads to multiple-valued solutions, i.e., to wave breaking [see *Whitham*, 1974, section 2.10]. Such feature of the solution is artificially removed by the linearization procedure performed by *Friedrichs and Aubrey* [1994], whereby a becomes a constant; in other words, we feel that linearization hides a fundamental feature of the kinematic wave approximation which may affect crucially tidal propagation in strongly dissipative and strongly convergent estuaries.

This point deserves some more thorough discussion in order to clarify the different viewpoint underlying the present approach as compared with that proposed by *Friedrichs and Aubrey* [1994]. Such different viewpoints have clearly emerged in the course of the revising this paper, also thanks to the contributions of C. T. Friedrichs.

In the present approach we do not make any assumption about the structure of U_0; we only know that U_0 is an $O(1)$ function periodic in time. In other words, we must allow for overtides to appear at leading order with any amplitude (a priori not small) and phase required

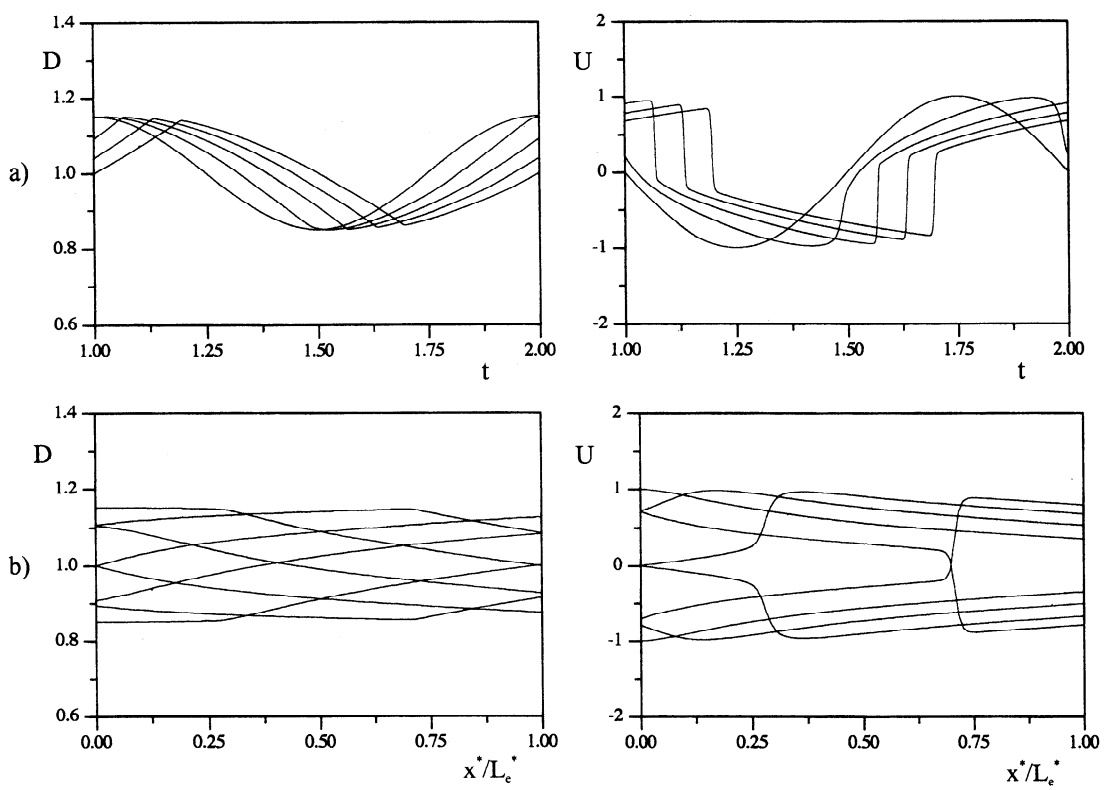

Figure 4. (a) Time evolution of the dimensionless flow depth $D = D^*/D_0^*$ and tidal velocity $U = U^*/U_0^*$ at distances $x^*/L_e^* = m/4$ $(m = 0, 4)$ from the outlet of the estuary as predicted by the kinematic wave equation (79) with a wave speed given by (81). (b) Spatial developments of D and U at times $t^*/T^* = m/8$ $(m = 1, 8)$. The values of the adopted parameters, typical of a strongly dissipative and strongly convergent estuary, are $\epsilon = 0.15$, $S = 1$, $R = 1$, $L_e^*/L_0^* = 2$.

to satisfy the nonlinear kinematic wave equation. In fact, if the product $U_0|U_0|$ is not linearized, (79) can be easily solved employing the method of characteristics. We have performed such calculation treating the frictional term by *Dronkers'* [1964] approach. Using the expansion (62), where $U_a(x)$ is now equal to 1, the wave speed $a(t)$ becomes

$$a(t) = \frac{15\pi}{16}\frac{1}{1+2U_0^2} \tag{81}$$

Equation (79) with $a(t)$ given by (81) has been solved numerically using the method of characteristics, marching in x by backward differences.

The temporal and spatial developments of the tidal wave obtained by such an approach are shown in Figure 4. Notice that cross sectionally averaged velocity and free surface have a 90° phase lag at the entrance of the estuary. The process of peaking emerges clearly from the spatial development of the temporal distribution of tidal velocity in a tidal cycle. It is less evident in the corresponding plot for free surface elevation. In other words, peaking does not necessarily show up in the form of breaking of the free surface as the developing discontinuity affects the velocity distribution more sharply than it affects free surface elevation. The above solution shows that the effect of overtides must be included at leading order as it gives rise to an $O(1)$ distortion of the tidal wave.

Friedrichs and Aubrey [1994], on the other hand, consider linearization of the frictional term as part of an expansion of the complete de Saint Venant equations. The latter viewpoint essentially assumes that, at leading order, U_0 simply reduces to the fundamental tidal component and higher harmonics have increasingly smaller amplitudes. This allows Friedricks and Aubrey to employ the expansion (34) and neglect, at leading order, the effect of the third harmonics, which ranges about 1/5 of the fundamental. The former viewpoint does not make the latter assumption, and indeed, as is shown in section 7, the fully nonlinear numerical solution of the complete de Saint Venant equation confirms that such assumption is not reasonable in the present case, as the full equations predict a development of the tidal wave that strongly resembles that predicted by the nonlinear kinematic wave approach.

7. Strongly Dissipative and Strongly Convergent Estuaries: a Nonlinear Parabolic Model

The results obtained by the kinematic wave model discussed in the previous section show that the approximations on which such approach is based are not uniformly valid; in fact, the process of peaking eventually leads to local values of the spatial derivatives ($U_{0,x}$) which are much larger than one would estimate from the choice of the spatial scale L_0^* made in section 6.

We now show that the process of peaking is partially damped by keeping the contribution proportional to $U_{0,x}$ in the equation of flow continuity at leading order. Such scheme is reasonable for estuaries like the Potomac (see Table 1) where the parameter $\mathcal{F}$ attains a value (1.66) comparable with the value of K (1.09).

The following equations then arise at leading order:

$$d_{0,t} + \mathcal{F}U_{0,x} - U_0 = 0 \tag{82}$$

$$d_{0,x} + U_0|U_0| = 0 \tag{83}$$

The latter system is readily reduced to a single nonlinear parabolic equation for U_0:

$$U_{0,xx} - \mu U_{0,x} - \mu(|U_0|U_0)_{,t} = 0 \tag{84}$$

where

$$\mu = \frac{1}{\mathcal{F}} \tag{85}$$

Equation (84) has been solved numerically with the following boundary condition at the mouth of the estuary:

$$(U_{0,x} - \mu U_0)_{x=0} = -\mu d_{0,t} \tag{86}$$

while the condition of vanishing velocity has been employed at the inner end of the estuary.

We have analyzed the propagation of a monochromatic tide by comparing the results based on the kinematic wave approach, which have been discussed in section 6, with the numerical solution of the nonlinear parabolic model at first order and with the numerical solution of the fully nonlinear de Saint Venant equations. The numerical solution of the parabolic model was obtained using an implicit scheme based on a six-point rectangular box where convective terms were discretized by using the SMART algorithm proposed by *Gaskell and Lau* [1988], while time derivatives were weighted averages in space of forward differences. The value chosen for the temporal weight θ was 0.5.

The numerical solution of the full de Saint Venant equations was obtained employing the classical box scheme developed by *Preissman* [1961]. We recall that such implicit scheme is based on a four-point rectangular box where time and spatial derivatives are discretized as weighted averages of differences calculated at adjacent points with temporal weight θ and spatial weight ψ. The values chosen for θ and ψ were 0.6 and 0.5 respectively.

Figures 5-7 show the temporal evolution of the dimensionless flow depth D and tidal velocity U at various dimensionless distances x^*/L_e^* from the outlet of the estuary, as predicted by the full de Saint Venant equations and by the nonlinear parabolic model for three sets of values of the parameters $\epsilon, S, \mathcal{F}$, and K. The spatial distributions of the maximum and minimum tidal elevations are also shown. The amplitude parameter ϵ was set equal to 0.15, a realistic value, sufficiently small to ensure that our expansion in powers of ϵ should apply. The value of the ratio L_e^*/L_0^* was set equal to 2,

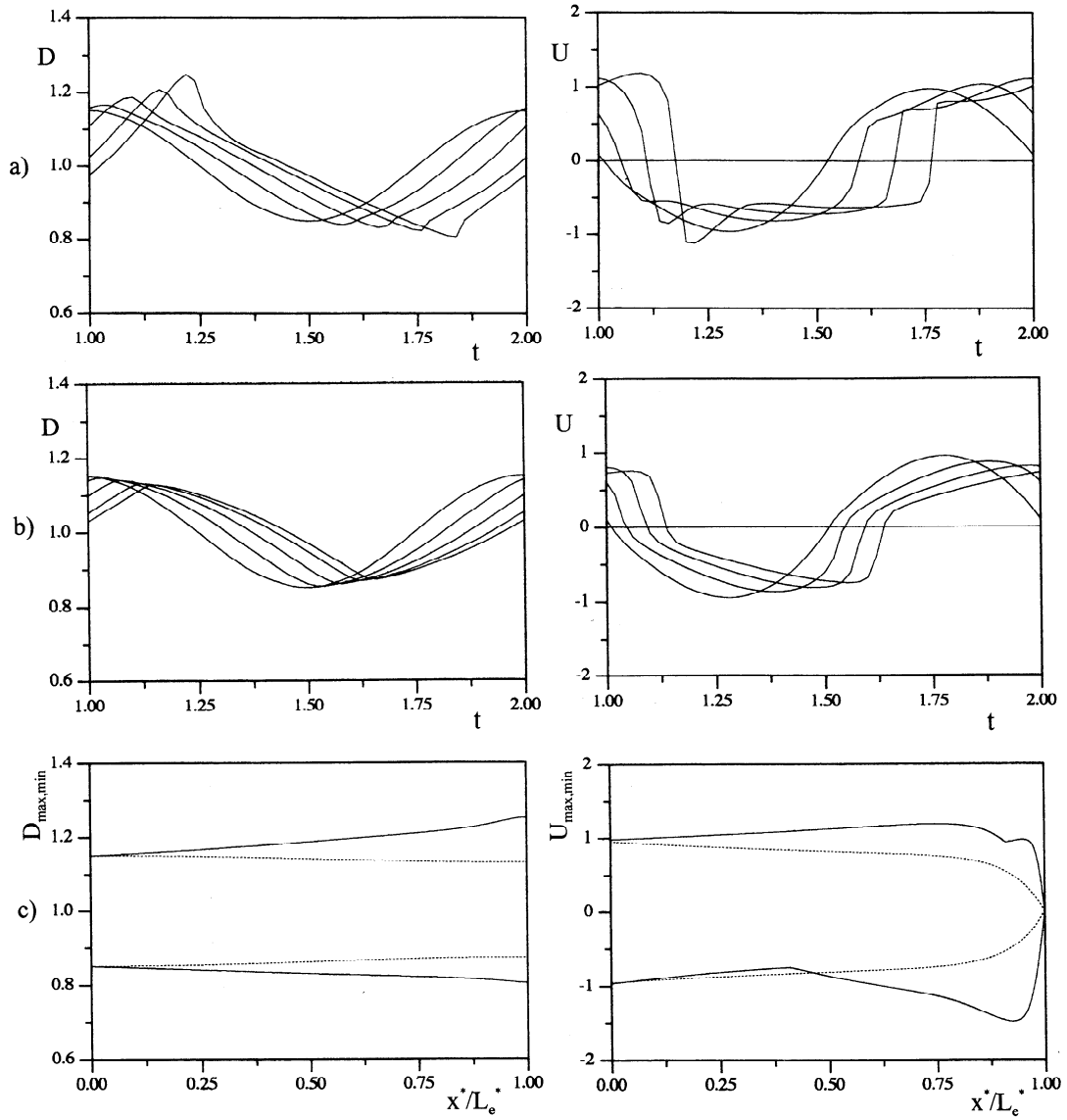

Figure 5. Time evolution of the dimensionless flow depth $D = D^*/D_0^*$ and tidal velocity $U = U^*/U_0^*$ at distances $x^*/L_e^* = m/4$ $(m = 0, 4)$ from the outlet of the estuary as predicted by (a) complete de Saint Venant equations, and (b) parabolic model at first order. (c) Maximum and minimum values of D and U along the estuary as predicted by complete de Saint Venant equations (solid line), and parabolic model at first order (dotted lines). The values of the adopted parameters, typical of a strongly dissipative and strongly convergent estuary, are $\epsilon = 0.15$, $S = 0.15$, $\mathcal{F} = 0.15$, $K = 1$, $R = 1$, $L_e^*/L_0^* = 2$.

though the latter choice is obviously inessential to the comparison presented herein.

The general comment that arises from a glance at Figures 5-7 is that the nonlinear parabolic model may be a good approximation of the full de Saint Venant solution for estuaries like the Potomac, i.e., when the relative effect of local inertia is sufficiently small and the effect of channel convergence is, at least partially, balanced by the effect of the $U_{0,x}$ term in the continuity equation (see Figure 7). The latter smooths the process of wave peaking and leads to damping of the tidal amplitude. Figure 7 also shows that the small effect of local inertia in the full de Saint Venant solution leads to a slight amplification of the tidal amplitude which, on the contrary, is slightly damped in the context of the parabolic model.

The weakly convergent and strongly dissipative limit is illustrated in Figure 8 where it appears that the solution based on the limit model of (72) agrees quite well with the full de Saint Venant solution. Both of them predict damping of the tidal wave and a phase lag between free surface elevation and tidal velocity somewhat smaller than $\pi/2$. Finally, we point out that, in agreement with *Jay* [1991], it turns out that the tidal wave speed increases as $\mathcal{F}$ increases.

Figures 5 and 6 also show that as $\mathcal{F}$ decreases, the

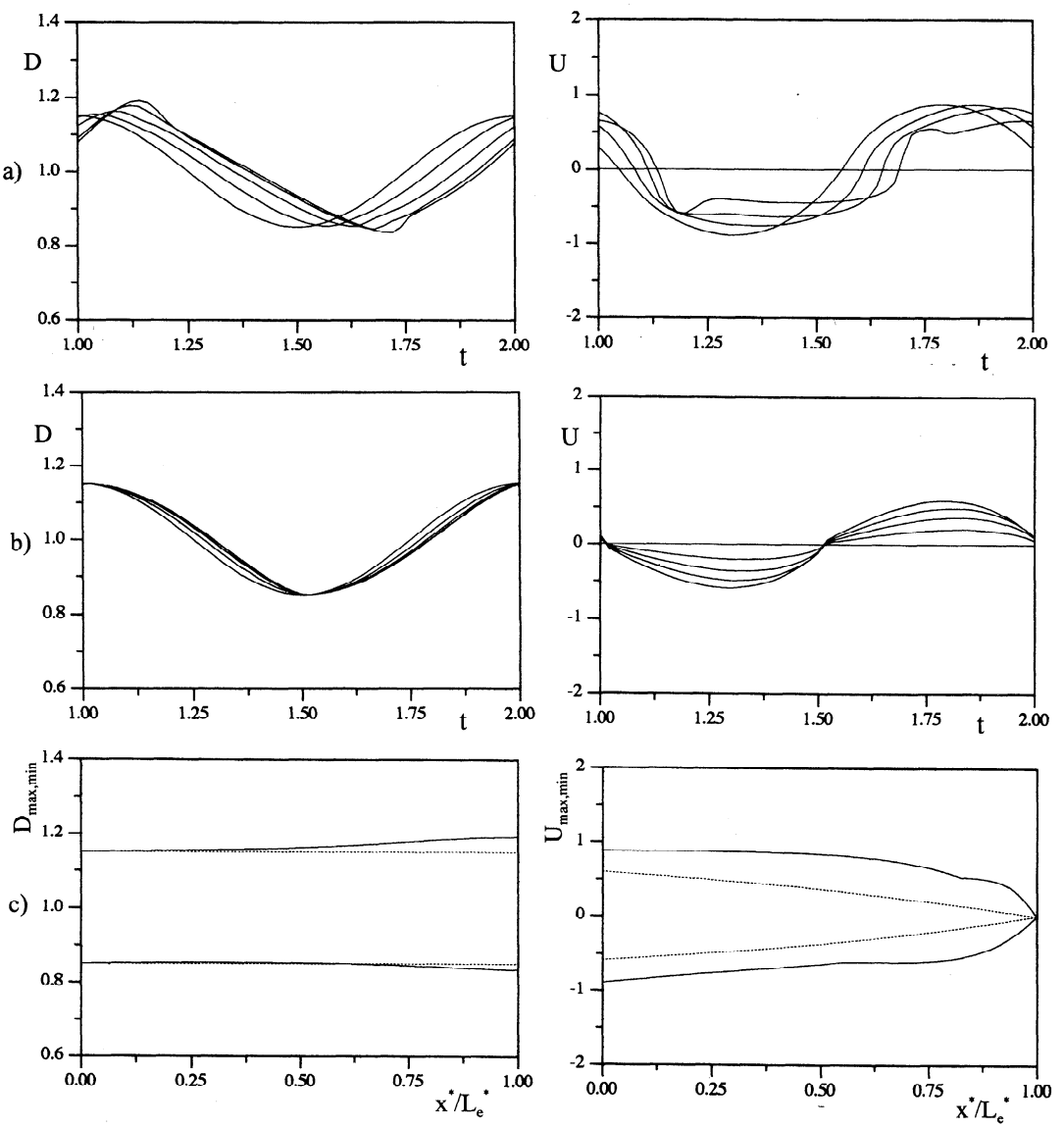

Figure 6. Time evolution of the dimensionless flow depth $D = D^*/D_0^*$ and tidal velocity $U = U^*/U_0^*$ at distances $x^*/L_e^* = m/4$ $(m = 0, 4)$ from the outlet of the estuary as predicted by (a) complete de Saint Venant equations, and (b) parabolic model at first order. (c) Maximum and minimum values of D and U along the estuary as predicted by complete de Saint Venant equations (solid line), and parabolic model at first order (dotted lines). The values of the adopted parameters, typical of a strongly dissipative and strongly convergent estuary, are $\epsilon = 0.15$, $S = 0.15$, $\mathcal{F} = 0.5$, $K = 1$, $R = 1$, $L_e^*/L_0^* = 2$.

agreement between the parabolic model and the full solution is less satisfactory. Notice that the process of peaking was predicted in the context of the kinematic wave approach and is also reproduced by the parabolic model, though the diffusive effect of the $U_{0,x}$ term in the continuity equation prevents the development of sharp discontinuities. The peaking process appears to be sharper in the solutions of the full de Saint Venant equations; this is mainly caused by the role of local inertia, as discussed in section 8. Also notice that the phase lag between free surface elevation and velocity of the tidal current ranges about 90° as in the kinematic model. It is appropriate to point out at this stage that somewhat similar patterns are also predicted by the combined first- and second-order solution of *Friedrichs and Aubrey* [1994].

8. The Effect of Local Inertia in Moderately Dissipative Estuaries

A glance at Table 1 shows that the effect of local inertia is seldom actually negligible in real estuaries. Figure 9 shows that, as the parameter S is increased starting from the strongly convergent and strongly dis-

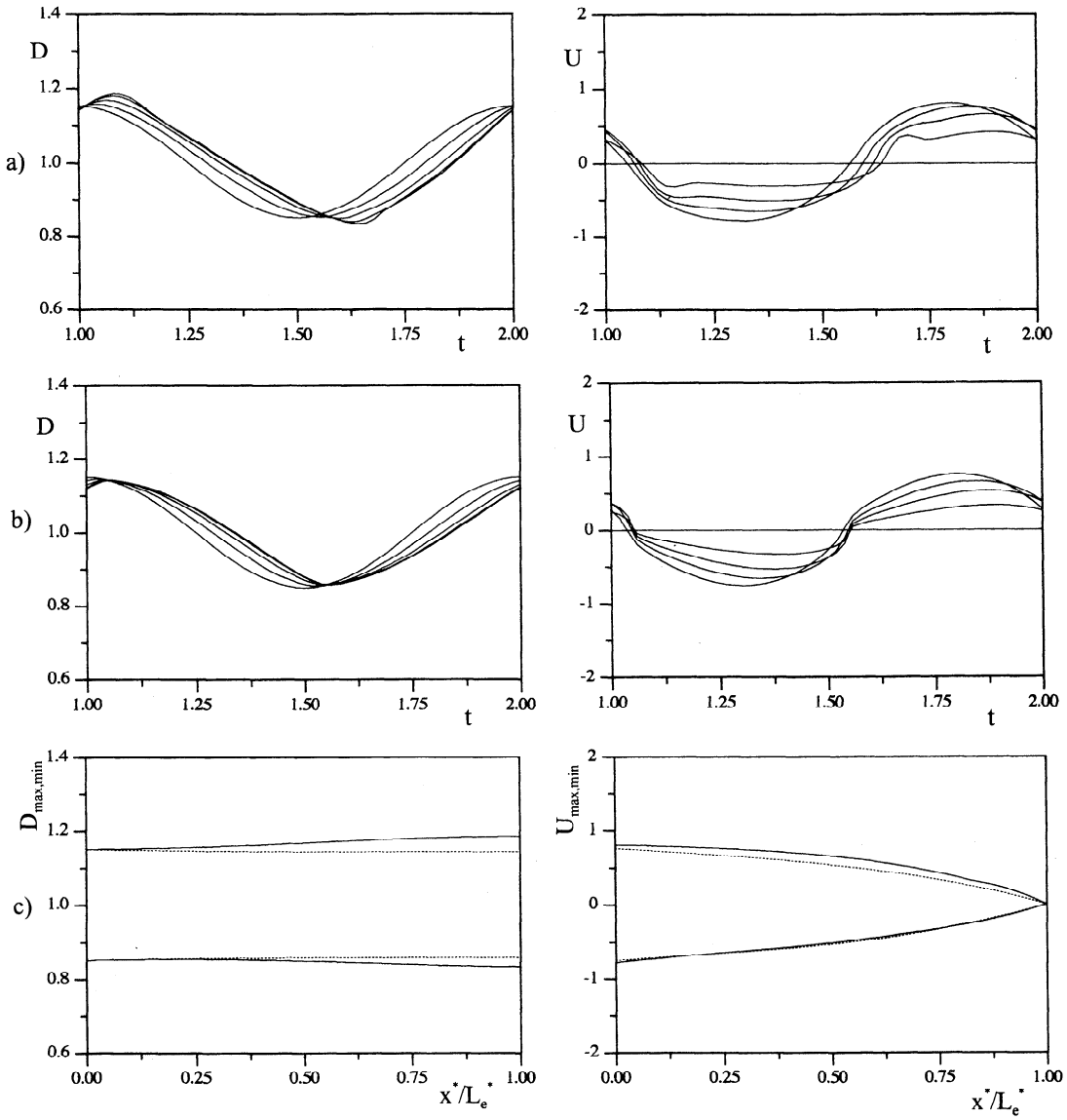

Figure 7. Time evolution of the dimensionless flow depth $D = D^*/D_0^*$ and tidal velocity $U = U^*/U_0^*$ at distances $x^*/L_e^* = m/4$ ($m = 0, 4$) from the outlet of the estuary as predicted by (a) complete de Saint Venant equations, and (b) parabolic model at first order. (c) Maximum and minimum values of D and U along the estuary as predicted by complete de Saint Venant equations (solid line), and parabolic model at first order (dotted lines). The values of the adopted parameters, typical of a strongly dissipative and moderately convergent estuary, are $\epsilon = 0.15$, $S = 0.15$, $\mathcal{F} = 1$, $K = 1$, $R = 1$, $L_e^*/L_0^* = 2$.

sipative case ($R = 1, K = 1, S = 0.15$ of Figure 5), the process of peaking of the tidal profiles is enhanced and the amplitude of the tidal wave is progressively more amplified. Hence local inertia plays a role opposite to that of the diffusive term $\mathcal{F}U_{0,x}$ of the continuity equation.

As regards ebb versus flood dominance, Figures 5-9 suggest that both strongly and moderately dissipative estuaries are invariably flood dominated. This is further confirmed by Figure 10, where the temporal development of the unit discharge throughout the tidal cycle is plotted for each of the cases corresponding to Figures 5-9.

9. Discussion and Conclusions

The analysis and results of the present paper suggest that modeling tide propagation in convergent estuaries by one-dimensional models requires some care in the choice of the simplest suitable model able to capture the fundamental physics of the process. In weakly dissipative estuaries the effect of convergence can be readily incorporated in the context of classical perturbation expansion approaches adequate to weakly nonlinear processes, with some care to treat the secular terms that may arise if an infinite domain is assumed in the model. The cascade process whereby overtides

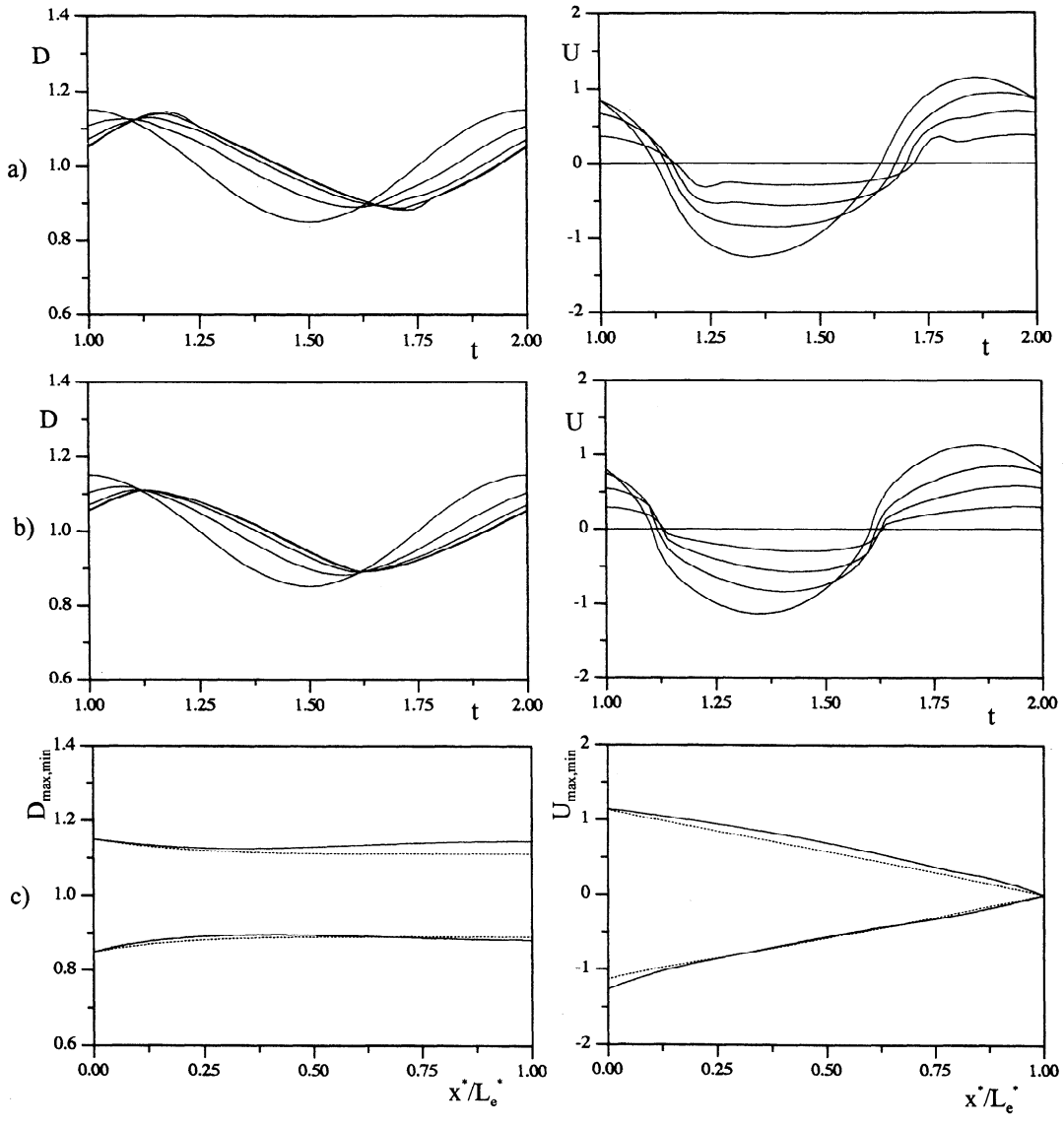

Figure 8. Time evolution of the dimensionless flow depth $D = D^*/D_0^*$ and tidal velocity $U = U^*/U_0^*$ at distances $x^*/L_e^* = m/4$ $(m = 0, 4)$ from the outlet of the estuary as predicted by (a) complete de Saint Venant equations, and (b) parabolic model at first order. (c) Maximum and minimum values of D and U along the estuary as predicted by complete de Saint Venant equations (solid line), and equation (72) (dotted lines). The values of the adopted parameters, typical of a strongly dissipative and weakly convergent estuary, are $\epsilon = 0.15$, $S = 0.15$, $\mathcal{F} = 1$, $K = 0.15$, $R = 1$, $L_e^*/L_0^* = 2$.

are generated and evolve landward is then analytically predicted and describe a tidal wave which is increasingly distorted as channel convergence increases. Furthermore, ebb dominance results along with the nonlinear generation of a seaward directed residual current. The latter result appears to be of some interest for possible applications to the dispersion of passive tracers in such estuaries. The linearized results of *Jay* [1991] concerning tidal wavenumber and tidal wave speed, respectively decreasing and increasing up to the critical convergence threshold, are confirmed by the present analysis.

In strongly dissipative estuaries the highly nonlinear nature of the frictional term gives rise to some distinct features that cannot be appropriately modeled by perturbation expansions which do not keep the strongly nonlinear nature of the mathematical problem at the leading order of approximation. In particular, according to our results, the linearized kinematic wave approximation derived at leading order by *Friedrichs and Aubrey* [1994] hides the tendency to breaking intrinsic to the full kinematic wave model. The perturbation expansion developed in this paper shows that it is possible to remove the restrictions posed by the linearized kinematic wave approximation, keeping the nonlinear nature of the problem, and provided allowance is made for some diffusion arising from the convective term of

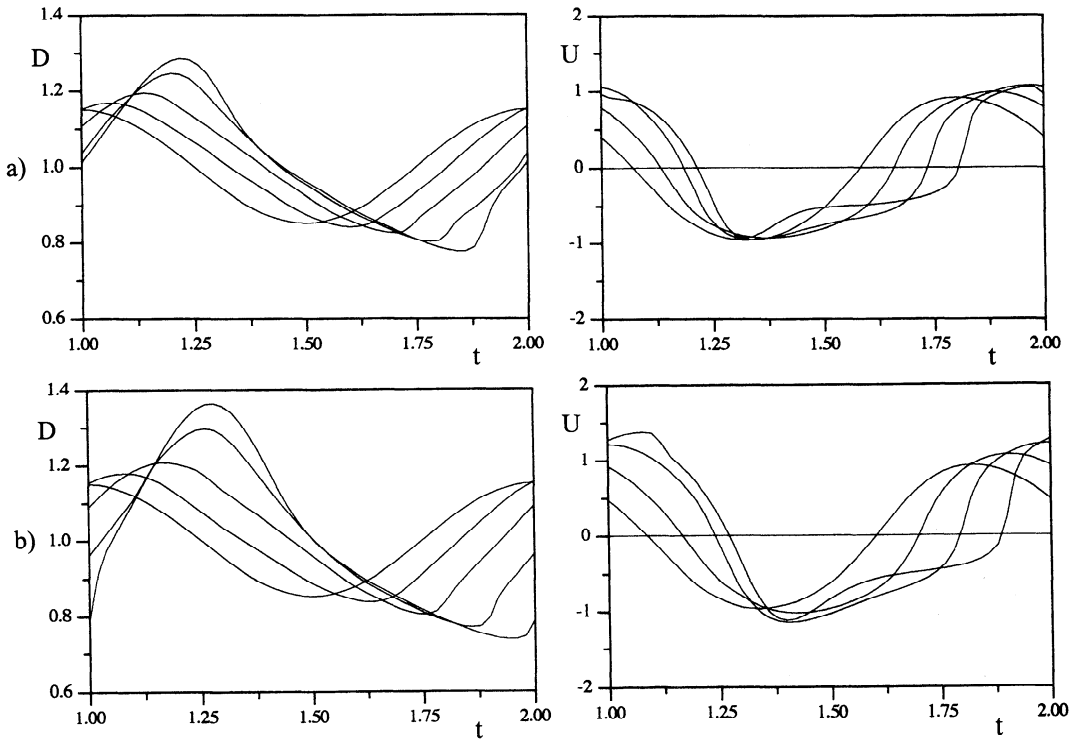

Figure 9. Time evolution of the dimensionless flow depth $D = D^*/D_0^*$ and tidal velocity $U = U^*/U_0^*$ at distances $x^*/L_e^* = m/4$ $(m = 0, 4)$ from the outlet of the estuary as predicted by the complete de Saint Venant equations. The values of the adopted parameters, typical of a moderately dissipative and strongly convergent estuary, are (a) $\epsilon = 0.15$, $S = 0.5$, $\mathcal{F} = 0.5$, $K = 1$, $R = 1$, $L_e^*/L_0^* = 2$, and (b) $\epsilon = 0.15$, $S = 0.8$, $\mathcal{F} = 0.5$, $K = 1$, $R = 1$, $L_e^*/L_0^* = 2$.

the continuity equation. The nonlinear parabolic model thus derived smooths the tendency to peaking of the nonlinear kinematic wave model. Comparison with solutions of the full de Saint Venant equations reveals that the parabolic approximation is appropriate, provided local inertia is sufficiently small while channel convergence is sufficiently strong. The former condition is quite severe and requires that the estuary be shallow and strongly dissipative. The latter condition, say $K \sim O(1)$, recalling (12), may be written in the form

$$\frac{L_b^*}{U_0^*} \sim 0\left(\frac{1}{c\omega^*}\right) \tag{87}$$

Hence, the time taken by the flow to travel along a reach of the tidal channel of length comparable with the convergence length must be small compared with the tidal period. This requirement is often satisfied in real convergent estuaries as shown in Table 2.

The significant distortion of the current profile typical of strongly dissipative estuaries has been invariably found to be associated with flood dominance. Furthermore, proceeding from the weakly convergent to the strongly convergent case, strongly dissipative estuaries display increasing values of the tidal wave speed and of the phase lag between free surface elevation and tidal velocity, as occurred in the context of *Jay's* [1991] work.

The above findings are based on several simplifying assumptions. It may be useful to summarize them. (1) The cross section has been assumed to be rectangular and the possible presence of tidal flats has been ignored. (2) The channel axis has been taken to be straight. (3) The bottom of the channel was fixed and horizontal. (4) Spatial and temporal variations of the friction coefficient have been ignored. (5) River discharge has been assumed to be negligible.

Most of these assumptions are not essential to the analysis performed herein. However, the retarding effect of tidal flats may significantly alter the picture displayed by the present results. In particular, it has been shown that, owing to the effects of tidal flats, the flood dominance typical of strongly dissipative estuaries may be converted into ebb dominance [*Speer and Aubrey*, 1985; *Friedrichs and Madsen*, 1992; *Shetye and Gouveia*, 1992]. This feature will require attention in order to be able to capture the controlling mechanisms of the morphodynamical equilibrium of environments like Venice lagoon, which is one of our final aims. This issue is the subject of a current investigation that is still in progress (S. Lanzoni and G. Seminara, manuscript in preparation, 1998).

The effects of a significant river discharge may sharply alter the tidal dynamics. In the context of the

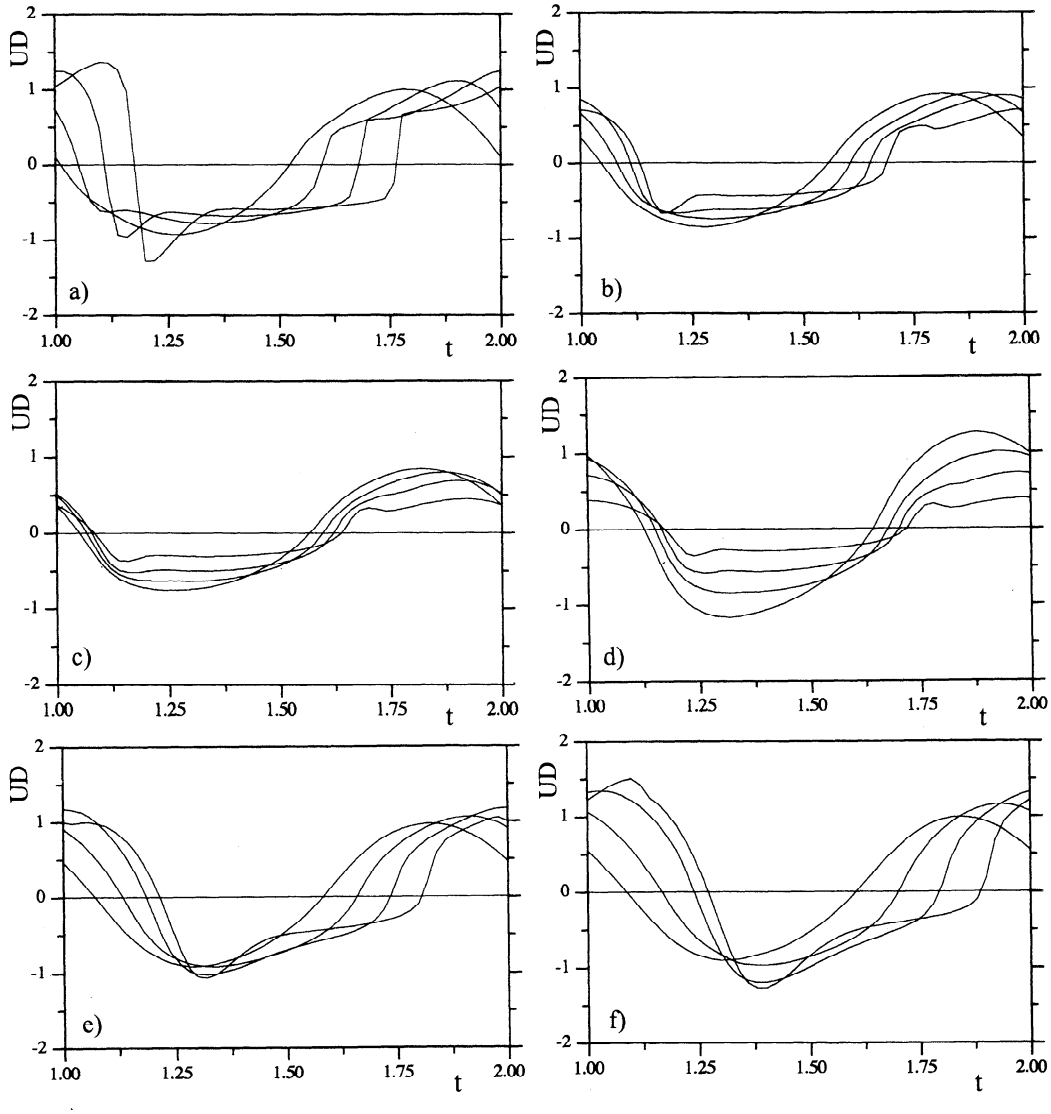

Figure 10. Time evolution of the dimensionless flow discharge per unit width UD as predicted by the complete de Saint Venant equations for the cases reported in (a) Figure 5, (b) Figure 6, (c) Figure 7, (d) Figure 8, (e) Figure 9a, and (f) Figure 9b.

linearized treatment of *Jay* [1991] it turns out that when river flow dominates the tide, both the damping rate of tidal amplitude and the tidal wavenumber are proportional to the square root of river speed. In other words, tidal wavelength and tidal wave speed decrease while tidal amplitude decays more rapidly upstream as river discharge increases. The above finding is true for almost the entire length of the Fraser and Columbia estuary and applies to a major section of the St. Lawrence [*Godin*, 1991].

As regards to assumption 3 one can readily appreciate that one of the effects of a reduction of flow depth in the landward direction is to enhance the effect of channel convergence. In fact, assume, for the sake of simplicity, that the average flow depth varies exponentially in the form $D_0^* \exp(-x^*/L_d^*)$, with L_d^* denoting a depth reduction length scale. Then some simple algebra shows that (10) and (11) still hold, provided (1) the expansion (9) is replaced by

$$D = D_0^* \left[D_0(x) + \epsilon d(x) \right] , \tag{88}$$

where

$$D_0(x) = \exp\left(-\frac{x^*}{L_d^*}\right) = \exp\left(-\frac{L_0^*}{L_d^*} x\right) , \tag{89}$$

and (2) the convergence parameter K (see (12)) is modified as follows:

$$K = \frac{U_0^*}{\epsilon \omega^*} \left(\frac{1}{L_b^*} + \frac{1}{L_d^*} \right) . \tag{90}$$

However, decreasing the average flow depth also leads to an increasing value of the ratio R/S; in other words, estuaries that are weakly dissipative in the outer region may turn into moderately or strongly dissipative progressing in the landward direction. For example, this is the case of the transition between the Bristol Channel, which is weakly dissipative, and the Severn Estuary, which is moderately/strongly dissipative.

Further, more subtle effects may arise as a result of spatial-temporal variations of roughness, possibly due to the presence of small-scale bed forms, such as dunes, whose characteristics are subject to oscillations throughout the tidal cycle. However, implementing such a correction will preliminarily require a thorough understanding of the mechanics of formation and development of estuarine bed forms, a subject that is still at an infant stage. Some steps in this direction, concerning large-scale bed forms, have been recently pursued [*Seminara and Tubino*, 1996].

Finally, curvature effects on the flow structure have so far been ignored but will require significant attention in order to predict the large-scale morphodynamics of real estuaries.

Appendix

Coefficients of (63), (65) are

$$\Delta_1 = \frac{\beta_1 + i\beta_2}{(1 - \mathcal{F}\lambda_1^2) - i\lambda_1} \quad \text{(A1)}$$

$$\Delta_2 = \frac{\delta_0 + i\delta_1}{4(1 - \mathcal{F}\lambda_1^2) - i2\lambda_1} \quad \text{(A2)}$$

$$\Delta_3 = \frac{\beta_3 + i\beta_3}{9(1 - \mathcal{F}\lambda_1^2) - i3\lambda_1} \quad \text{(A3)}$$

$$\phi_1 = -\left(\frac{\Delta_1}{\mathcal{F}} + r\gamma_0\Gamma_1\right) + i\left(\lambda_1\Delta_1 - r\gamma_1\Gamma_1\right) \quad \text{(A4)}$$

$$\phi_2 = -\left(\frac{\Delta_2}{\mathcal{F}} + 2\gamma_0\Gamma_1\lambda_1\mathcal{F} + \frac{\gamma_0^2 - \gamma_1^2}{2}\right) + i\left(2\lambda_1\Delta_2 - \gamma_0\gamma_1 + \lambda_1\mathcal{F}(\gamma_0^2 - \gamma_1^2)\right) \quad \text{(A5)}$$

$$\phi_3 = -\left(\frac{\Delta_3}{\mathcal{F}} + r\gamma_3\Gamma_3\right) + i\left(3\lambda_1\Delta_3 - r\gamma_4\Gamma_3\right) \quad \text{(A6)}$$

$$\varphi_j = \frac{\Delta_j}{2\mathcal{F}} - i\left(\lambda_j\Delta_j\right) \qquad (j = 1, 3) \quad \text{(A7)}$$

where

$$\beta_1 = -r\lambda_1\mathcal{F}\gamma_1\Gamma_1 \qquad \beta_2 = r\lambda_1\mathcal{F}\gamma_0\Gamma_1$$

$$\beta_3 = -3r\lambda_1\mathcal{F}\gamma_4\Gamma_3 \qquad \beta_4 = 3r\lambda_1\mathcal{F}\gamma_3\Gamma_3$$

$$\gamma_3 = \lambda_1^3 - \frac{3}{4}\frac{\lambda_1}{\mathcal{F}^2} \qquad \gamma_4 = \frac{3}{2}\frac{\lambda_1^2}{\mathcal{F}} - \frac{1}{8\mathcal{F}^3}$$

$$\delta_0 = 2\lambda_1\mathcal{F}\left[(\gamma_0 - \gamma_0\gamma_1) + (\lambda_1\mathcal{F}(\gamma_0^2 - \gamma_1^2)\right]$$

$$\delta_1 = 2\lambda_1\mathcal{F}\left[\gamma_1 + 2\lambda_1\mathcal{F}\gamma_0\gamma_1 + \frac{\gamma_0^2 - \gamma_1^2}{2}\right]$$

$$\Gamma_1 = \frac{16}{15\pi}\hat{U}_a\left[1 + \frac{6}{\hat{U}_a^2}\left(\frac{\lambda_1^2}{4} + \frac{1}{16\mathcal{F}^2}\right)\right] \qquad \Gamma_3 = \frac{4}{15\pi}\frac{1}{\hat{U}_a}$$

Acknowledgments. This work has been financially supported by the Italian Ministry of Scientific Research (MPI 40%, National Project "Trasporto di sedimenti e evoluzione morfologica di corsi d'acqua, estuari e lagune alle diverse scale temporali"). We thank the two referees, C. T. Friedrichs and D. A. Jay for constructive criticism of the present work, which has resulted in considerable improvement over the original version of the paper.

References

Abraham, G., P. de Jong, and F. E. van Kruiningen, Large-scale mixing processes in a partly mixed estuary, in *Physics of Shallow Estuaries and Bays*, edited by J. van de Kreeke, pp. 6-21, Springer-Verlag, New York, 1986.

Allen, G. P., J. C. Salomon, P. Bassoulet, Y. Du Penhoat, and C. De Grandpré, Effects of tides in mixing and suspended sediment in macrotidal estuaries, *Sediment. Geol., 26*, 69-90, 1980.

Ages, A., and A. Woollard, The tides in the Fraser estuary, *Pac. Mar. Sci. Rep. 76-5*, 100 pp., Inst. of Ocean Sci., Patricia Bay, B.C., 1976.

de Jong, H., and F. Gerritsen, Stability parameters of western Scheldt estuary, in *Proc. 19th Int. Conf. Coastal Eng.*, New York, American Society of Civil Engineers, 3078-3093, 1984.

Dronkers, J. J., *Tidal Computations in Rivers and Coastal Waters*, 518 pp., North-Holland, New York, 1964.

Duwe, K. C., and J. Sündermann, Currents and salinity transport in the lower Elbe estuary: Some experiences from observations and numerical simulation, in *Physics of Shallow Estuaries and Bays*, edited by J. van de Kreeke, pp. 30-39, Springer-Verlag, New York, 1986.

Friedrichs, C. T., and D. G. Aubrey, Tidal propagation in strongly convergent channels, *J. Geophys. Res., 99*, 3321-3336, 1994.

Friedrichs, C. T., and O. S. Madsen, Nonlinear diffusion of the tidal signal in frictionally dominated embayments, *J. Geophys. Res., 97*, 5637-5650, 1992.

Gaskell, P. H., and A. K. C. Lau, Curvature-compensated convective transport: SMART, a new boundedness preserving transport algorithm, *Int. J. Numer. Methods Fluids, 8*, 617-641, 1988.

Giese, B.S., and D. A. Jay, Modelling tidal energetics of the Columbia river estuary, *Estuarine Coastal Shelf Sci., 29*, 549-571, 1989.

Godin, G., Frictional effects in river tides, in *Tidal Hydrodynamics*, edited by B.B. Parker, pp. 379-402, John Wiley, New York, 1991.

Green, G., On the motion of waves in a variable canal of small depth and width, *Trans. Cambridge Philos. Soc., 6*, 457-462, 1837.

Greenberg, D.A., A numerical model investigation of tidal phenomenon in the bay of Fundy and Gulf of Maine, *Mar. Geod., 2*, 161-187, 1979.

Jay, D. A., Green's law revisited: Tidal long-wave propagation in channels with strong topography, *J. Geophys. Res., 96*, 20,585-20,598, 1991.

Knight, D. W., Some field measurements concerned with the behaviour of resistance coefficients in a tidal channel, *Estuarine Coastal Shelf Sci., 12*, 303-322, 1981.

Kreiss, H., Some remarks about nonlinear oscillations in tidal channels, *Tellus, 9*, 53-68, 1957.

Le Blond, P. H., On tidal propagation in shallow rivers, *J. Geophys. Res., 83*, 4717-4721, 1978.

Lewis, R. E., and J. O. Lewis, Shear stress variations in an estuary, *Estuarine Coastal Shelf Sci., 25*, 621-635, 1987.

Lightill, J., *Waves in Fluids*, pp. 89-136, Cambridge Univ. Press, New York, 1978.

Nayfeh, A. H., *Perturbation Method*, John Wiley, New York, 1973.

Parker, B. B., The relative importance of the various nonlinear mechanisms in a wide range of tidal interactions, in

Tidal Hydrodynamics, edited by B. B. Parker, pp. 236-268, John Wiley, New York, 1991.

Prandle, D., and N. L. Crookshank, Numerical model of St. Lawrence river estuary, *J. Hydraul. Div. Am. Soc. Civ. Eng., 100*, 517-529, 1974.

Prandle, D., and M. Rahman, Tidal response in estuaries, *J. Phys. Oceanogr., 10*, 1552-1573, 1980.

Preissman, A., Propagation des intumescenes dans les canaux et riviers, paper presented at 1st Congress de l'Association Francaise de Calcul, Grenoble, France, 1961.

Robinson, I. S., L. Warren, and J. F. Longbottom, Sea-level fluctuations in the Fleet, an english tidal lagoon, *Estuarine Coastal Shelf Sci., 16*, 651-668, 1983.

Seminara, G., and M. Tubino, On the formation of estuarine free bars, paper presented at Physics of Estuaries and Coastal Seas (PECS), The Hague, Netherlands, September 1996.

Shetye, S. R. G., and A. D. Gouveia, On the role of geometry of cross-section in generating flood-dominance in shallow estuaries, *Estuarine Coastal Shelf Sci., 35*, 113-126, 1992.

Speer, P. E., and D. Aubrey, A study of non-linear tidal propagation in shallow inlet/estuarine systems, II, Theory, *Estuarine Coastal Shelf Sci., 21*, 206-240, 1985.

Thatcher, M. L., and D. R. F. Harleman, A mathematical model for the prediction of unsteady salinity in estuaries, *Rep. 144*, 232 pp., Dept. Civ. Eng., Mass. Inst. of Technol., Cambridge, 1972.

Uncles, R. J., A note on tidal asymmetry in the Severn estuary, *Estuarine Coastal Shelf Sci., 13*, 419-432, 1981.

Uncles, R. J., M_4 tides in a macrotidal, vertically mixed estuary: The Bristol Channel and Severn, in *Tidal Hydrodynamics*, edited by B. B. Parker, pp. 341-355, John Wiley, New York, 1991.

Wallis, S. G., and D. W. Knight, Calibration studies concerning a one-dimensional numerical tidal model with particular reference to resistance coefficient, *Estuarine Coastal Shelf Sci., 19*, 541-562, 1984.

Whitham, G. B., *Linear and nonlinear waves*, John Wiley, New York, 1974.

Wright, L. D., J. M. Coleman, and B. C. Thom, Processes of channel development in a high-tide-range environment: Cambridge Gulf-Ord river Delta, Western Australia, *J. Geol., 81*, 15-41, 1973.

S. Lanzoni, Dipartimento di Ingegneria Idraulica Marittima e Geotecnica, Università di Padova, Via Loredan, 20, 35131 Padua, Italy. (e-mail: lanzo@idra.unipd.it)

G. Seminara, Istituto di Idraulica, Università di Genova, Via Montallegro, 1, 16145 Genoa, Italy. (e-mail: sem@idra.unige.it)

(Received January 29, 1997; revised July 27, 1998; accepted August 31, 1998.)